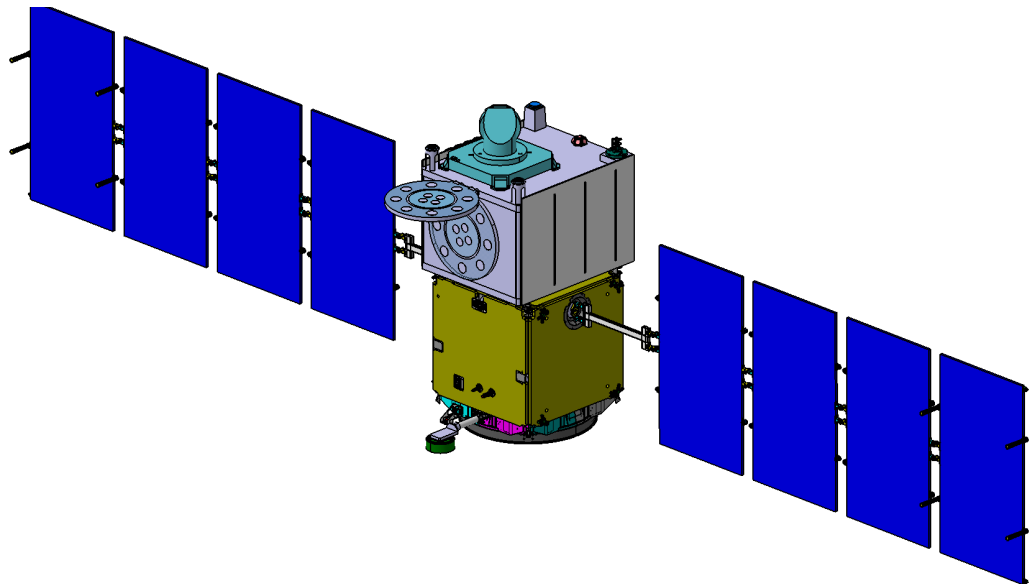


STE-QUEST

(Space-Time Explorer and
Quantum Equivalence Principle Space Test)

A class M mission proposal for Cosmic Vision 2015-2025



Proposal contact details

Science Team

K. Bongs, University of Birmingham, UK
 P. Bouyer, IOTA, France
 W. Ertmer, IQ, Leibniz Universität Hannover, Germany
 R. Holzwarth, Max-Planck Insitutit für Quantenoptik, Germany
 L. Iess, Università LaSapienza, Italy
 A. Landragin, Observatoire de Paris, France
 P. Laurent, Observatoire de Paris, France
 E. Rasel, IQ, Leibniz Universität Hannover, Germany
 C. Salomon, LKB, France
 S. Schiller, University of Düsseldorf, Germany
 U. Sterr, PTB, Germany
 G. Tino, LENS, University of Firenze, Italy
 P. Wolf, Observatoire de Paris, France

Supporters

A. Clairon, Observatoire de Paris, France	C. Oates, NIST, USA
P. Lemonde, Observatoire de Paris, France	M. Kasevich, Stanford, USA
S. Reynaud, LKB, France	J. Ye, JILA, NIST, University of Colorado, USA
J-M. Courty, LKB, France	A. Madej, NRC, Canada
H. Dittus, DLR, Germany	L. Marmet, NRC, Canada
C. Lämmerzahl, ZARM, University of Bremen, Germany	J. Thomsen, Niels Bohr Institute, Denmark
S. Theil, ZARM, University of Bremen, Germany	U. Johann, Astrium, Germany
F. Riehle, PTB, Germany	A. Rathke, Astrium, Germany
E. Peik, PTB, Germany	A. Görlitz, University of Düsseldorf, Germany
P. Gill, NPL, Great Britain	A. Peters, Humboldt University of Berlin, Germany
T.W. Hänsch, MPQ, Germany	R. Blatt, University of Innsbruck, Austria
T. Udem, MPQ, Germany	F. Vedel, Université de Provence, France
B. Christophe, ONERA, France	M-C. Angonin, Observatoire de Paris, France
B. Foulon, ONERA, France	P. Delva, ESA, Netherlands
M. Inguscio, LENS, University of Firenze, Italy	K. Sengstock, University of Hamburg
G. Modugno, LENS, University of Firenze, Italy	W. Schleich, University of Ulm, Germany
N. Poli, LENS, University of Firenze, Italy	R. Walser, TU Darmstadt, Germany
F. Levi, INRIM, Italy	J. Vigué, University Paul Sabatier, Toulouse, France
D. Calonico, INRIM, Italy	M. Arndt, Vienna, Austria
P. Berio, OCA, France	T. Damour, IHES, France
F. Bondu, OCA, France	Ch. Bordé, LPL, CNRS, Université Paris Nord, France
A. Brillet, OCA, France	L. Lusanna, INFN, Firenze, Italy
G. Metris, OCA, France	C. Braxmeier, Astrium, Germany
E. Samain, OCA, France	T. van Zoest, DLR, Germany
P. De Natale, INOA, Italy	S. Herrmann, ZARM, University of Bremen, Germany
O. Bertolami, IST, Portugal	D. Giuliani, ITP, University of Hannover, Germany
R. Bingham, RAL, Great Britain	J. Reichel, ENS, Paris
W. Seboldt, DLR, Germany	P. Thomann, University de Neuchatel, Swiss
L. Maleki, OEwaves Inc., USA	H. Müller, Berkeley, USA
N. Yu, JPL, USA	T. Pfau, University of Stuttgart
J.D. Anderson, Global Aerospace Corporation, USA	J. Müller, IFE, University of Hannover
K.T. Nock, Global Aerospace Corporation, USA	C. Jentsch, Astrium, Germany
J. Bergquist, NIST, USA	U. Schreiber, Wetzell, Germany
A. Nevsky, Düsseldorf, Germany	

With support from TIMETECH, TESAT, MENLO Systems

A Executive Summary

The Space-Time Explorer and Quantum Test of the Equivalence Mission (STE-QUEST) is devoted to a precise measurement of the effect of gravity on time and matter using an atomic clock and an atom interferometer. It tests a fundamental assumption and one of the most fundamental predictions of Einstein's Theory of General Relativity with high precision and thereby searches for hints of quantum effects in gravity, contributing to the exploration of one of the current frontiers in fundamental physics.

The Principle of Equivalence (EP), which is fundamental to our understanding and theoretical description of gravity, states that the gravitational field is equivalent to an accelerated frame, so that over a time interval a body builds up a velocity proportional to the acceleration of gravity. An observer will thus expect a Doppler shift in the tick rate of a clock, proportional to this velocity. Indeed, the Principle of Equivalence predicts a gravitational redshift of this amount. However, since this redshift in frequency is equivalent to a change of time intervals, this raises the necessity for describing gravitation through the curvature of space-time. The EP also postulates that gravitational acceleration is universal, independent of the type of body (universality of free fall). By combining matter-wave interferometry and clock timing in one mission, STE-QUEST tests two aspects of Einstein's Equivalence Principle with one mission.

The first primary goal of the mission will be to measure space-time curvature via the precise determination of gravitational time dilation, i.e. the difference in the tick rate of a clock when it is compared with a clock located at a different, usually distant, location. The most precise gravitational time dilation measurement in Earth's gravity field dates back to a 1976 rocket mission, where an accuracy of $\sim 10^{-4}$ was achieved. The ESA ACES mission on the ISS aims to improve this accuracy by approximately an order of magnitude. STE-QUEST aims to achieve a further improvement compared to ACES, by a factor between 45 and 400 (in the advanced STE-QUEST scenario), making use of a highly elliptic orbit and advanced atomic clocks. In addition, STE-QUEST will also perform a precise measurement the redshift due to Sun's gravitational field, thereby testing for the independence of the redshift on the nature of the mass producing the gravitational field. The improvement is a factor of approx. 20 compared to ACES. The measurement is performed by comparing ultra-precise ground clocks as they rotate with the Earth. The STE-QUEST satellite is hereby used as a relay station.

A second primary goal is a quantum test of the universality of free-fall. STE-QUEST will test the Universality of Free Fall by interferometrically tracking the propagation of matter waves in the Earth field, striving for an accuracy better than one part in 10^{15} .

The satellite payload consists of two instruments: a cold atom-based clock of highest performance and an atom interferometer. The clock is derived from the well-developed microwave clock PHARAO, which is also the core of the ACES mission. The performance of the clock is improved compared to the current implementation for ACES by an optically derived ultra-pure microwave signal and by using the more favourable atomic species Rubidium. During the mission, the tick rate of the space clock will be nearly continuously compared with atomic clocks on the Earth, using precise microwave frequency transfer methods similar to those developed for the ACES mission, as well as using a laser coherent link based on the successful LCT technology in use by ESA.

The atom interferometer will compare the free propagation of coherent matter waves of two isotopes of rubidium ($^{85}\text{Rb}/^{87}\text{Rb}$) under the influence of the Earth's gravity. The use of ultra-cold matter at quantum degeneracy will permit to go far beyond the current accuracy of tests. The atom interferometer is based on the strong European developments in this field, including the pre phase A studies in the ELIPS-3 programme "Space atom interferometer" (SAI), "Quantum gases in microgravity"(SpaceBEC), the DLR project QUANTUS (QUANTengase Unter Schwerelosigkeit) and the CNES project I.C.E. (Interférométrie Cohérente pour l'Espace).

The highly elliptic orbit of the satellite provides a large variation in the gravitational potential between perigee and apogee and maximizes the accuracy of the measurements of the redshift,. Clock and atom interferometer will operate alternately, in order to reduce power requirements. A mission duration of up to 5 years is intended.

In the advanced STE-QUEST scenario, the PHARAO clock can be replaced by an optical clock. This results in an improvement of the measurement accuracy by a factor 9 for the Earth redshift measurement.

Besides the fundamental physics results, the mission provides, at no additional cost, a new tool for mapping the gravitational potential on the Earth surface with high spatial resolution and at a high level of accuracy (1 cm equivalent height). This is achieved through the measurement of the differential gravitational shift between ground clocks, which is primarily used for the Sun redshift test. If a worldwide network of ground clocks will be available by the mission time. STE-QUEST will establish a global reference frame for the Earth's gravitational potential. This approach will complement current and future gravity space geodetic missions such as CHAMP, GRACE and GOCE as well as altimetry missions like JASON and Envisat in establishing the Global Geodetic Observing System (GGOS).

The STE-QUEST mission concept is derived from the STE assessment study by ESA's Concurrent Design Facility in June-July 2010, following the 2010 recommendations of ESA's Fundamental Physics Working Group. STE has been found to be compatible with the cost envelope of the Cosmic Vision call and to have manageable risks. In STE-QUEST, STE is extended by the inclusion of the atom interferometer instrument.

Many components and subsystems of the satellite payload have been developed up to engineering or flight models in the frame of the ESA ACES mission and other missions using lasers and optical techniques, and have technical readiness level of 6-8. In particular, the atomic clock PHARAO and the associated microwave link will have been validated in space on the ISS in 2014. The laser link is based on the currently operational LCT technology used by ESA.

Some subsystems are currently under development and are expected to reach TRL 5 by 2014, as required by the call. This includes the atom interferometer with the phase-locked laser system (currently tested on the 0-g Airbus, in the drop tower, and in 2013 on a sounding rocket), the frequency comb (to be flown on a sounding rocket in 2016), the optical link (ESA study announced), and the optical clock proposed for the advanced version of the mission. A complete hardware ensemble with a dual-species atom interferometer and a frequency comb will be launched on a sounding rocket in 2016 (MAIUS II). The goal performance of the optical clock for the advanced STE-QUEST scenario has nearly been achieved in a European laboratory by the time of submission of this proposal, and a breadboard version aiming for achieving the STE-QUEST specifications is under development for 2011 – 2014 in a EU-FP7-SPACE project.

B Introduction

Einstein's theory of General Relativity is a cornerstone of our current description of the physical world. It is used to describe the flow of time in presence of gravity, the motion of bodies ranging in size from satellites to galaxy clusters, the propagation of electromagnetic waves in the presence of massive bodies, and the dynamics of the universe as a whole. In general, the measurement of general relativistic effects is very challenging, due to their small size [Wil06]. Thus, most effects are known with limited accuracy; but some of its predictions have been tested with high accuracy, for example the time delay of electromagnetic waves via the Cassini mission [Ber01], and the existence of gravitational waves via binary stars pulsar radio emission (Nobel prize 1993). The accuracy of the determination of these effects is at the 20 ppm level.

Although General Relativity has been very successful so far, it as well as numerous other alternative or more general theories proposed in the course of the development of theoretical physics, are classical theories. As such, they are fundamentally incomplete, because they do not include quantum effects. In fact, it has not yet been possible to develop a theory of gravity that includes quantum mechanics in a satisfactory way, although enormous effort has been devoted to this goal. Such a theory would represent a crucial step towards a unified theory of all fundamental forces of Nature. Several approaches have been proposed and are currently under investigation (e.g. string theory). A full understanding of gravity will require observations or experiments that determine the relationship of gravity with the quantum world. This topic is a prominent field of activity, and includes the current studies of dark energy.

One approach towards a fuller understanding consists in testing the assumptions and predictions of General Relativity with precision experiments on the laboratory to solar system scale. The highest precision can be achieved by employing state-of-the-art technology. Two main experiments can be today be performed with strongly improved accuracy:

One of the most fascinating effects predicted by General Relativity and other metric theories of gravity is slowing of clocks in a gravitational field (gravitational time dilation). The comparison of frequencies of two identical clocks ticking at different locations x , x' is given, in the weak-gravitational-field-limit, by

$$\nu(x')/\nu(x) = 1 + (U(x') - U(x))/c^2, \quad (1)$$

$\nu(x')$ is the frequency of the clock located at x' , as observed at any other location, U is the gravitational potential, $U(x) = -GM/|x|$, in case of a spherically symmetric body of mass M . In short, time runs (or clocks tick) more slowly near a massive body. Stationary clocks and observers have been assumed in Eq.(1), for simplicity.

The gravitational time dilation was measured with 10^{-5} inaccuracy in the 1976 Gravity Probe-A experiment [Ves81] by comparing a ground clock with a clock on a rocket as the height changed. The most performing clocks available at the time, hydrogen masers, were used for this experiment. The ACES mission planned to fly on the ISS in 2014 seeks to improve the determination by a approximately 10, by using a cold atom clock (PHARAO) (the gain depends on the actual clock performance). The use of an optimized orbit as well as recent progress on cold atom clocks in the optical domain and in optical

technology enables a re-attack of this fundamental test with approximately 2 orders of magnitude better sensitivity.

The equivalence of gravitational and inertial mass is, together with Local Position Invariance, the Universality of the Gravitational Redshift and Local Lorentz Invariance, one of the cornerstones of general relativity. This equivalence results in the Universality of Free Fall: free fall is independent of test mass composition. The free fall universality is investigated with classical (bulk) matter e.g. in the Lunar Laser Ranging [Wil76] and torsion balance [Sch07] experiments and shows no deviation in parts of 10^{13} .

Tracking the free propagation of matter waves extends free fall experiments in the domain of quantum objects. We consider it as a conceptually different approach compared to all other free-fall tests based on classical bodies. According to quantum mechanics, particles have to be described as wave packets, which implies the concept of coherence of the different partial waves. Current debates on the interpretation of the measurements performed with matter waves emphasize these conceptual differences.

STE-QUEST is a fundamental physics mission dedicated to these two questions; its primary tasks are to measure the gravitational time dilation with unprecedented accuracy and to perform a quantum test of the universality of free fall, improving current tests with matter waves by six orders of magnitude.

Its results can be interpreted as tests of General Relativity and other metric theories of gravity and as tests for the existence of new fields associated to matter (see Sec. C). The outcome of the STE-QUEST mission will be either a confirmation of the foundations of General Relativity and of metric theories within the accuracy provided by the instruments, or the discovery of a deviation. In the latter case, the mission would provide a first indication of the breakdown of current (classical) gravitational physics theories and could pave the way towards a unified theory of all forces.

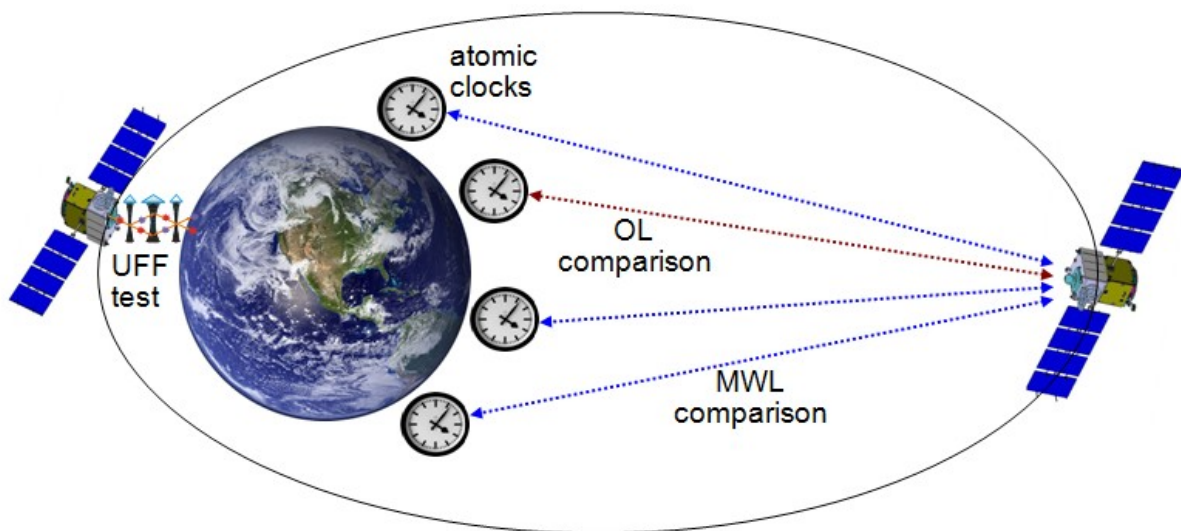


Figure B1: General concept of the STE-QUEST mission. The clock on the satellite is compared with one or more ground clocks as the satellite orbits earth on a highly elliptical orbit. During the perigee the local acceleration of two rubidium isotopes is measured and compared.

C Scientific objectives and requirements

Primary objectives

- High-precision measurement of the Earth gravitational time dilation (baseline inaccuracy: 1.6×10^{-7} , advanced STE-QUEST scenario with optical clock: 1.8×10^{-8})
- High-precision measurement of the Sun gravitational time dilation (inaccuracy 6×10^{-8})
These measurements search for the neutron's scalar charge, and test the anomalous coupling of matter to the Standard Model quantum fields
- Test of the universality of free fall for quantum objects at unprecedented level (inaccuracy: 1×10^{-15})

Secondary objectives

- Tests of Lorentz Invariance in the matter and photon sector (factor 20 improvement)
- Contribution towards establishing a new definition of the unit of time by allowing intercontinental comparisons of the most accurate future terrestrial clocks

- The evolution of coherent matter wave packets in a clean environment

Spin-off to other fields (outside fundamental physics)

- Comparison of distant terrestrial clocks at the level attained by the time of the mission (10^{-18} level or better)
- Establishment of a new approach to the determination of the geopotential, with 1 cm equivalent height resolution
- Demonstration of clock and link technology as well as high precision inertial sensors based on atom interferometers for future applications, e.g. in precision spacecraft navigation
- Demonstration on high performance real-time range determination with precision 25 times (based on code phase) to 1000 times (based on carrier phase) higher compared to systems onboard ERS-2 or TOPEX POSEIDON
- Comparison of 3 different orbit determination systems: Laser-Ranging, μm -precision Microwave Ranging, GPS-based orbit determination
- Monitoring stability of the Galileo/GPS/Glonass time scales

C.1 Gravitational time dilation measurement and search for new physics

C.1.1 Scientific Motivation

One primary science goal is a measurement and test of the gravitational time dilation in the weak-field limit, Eq.(1), as predicted by metric theories of gravitation. These theories also predict that the dilation is independent of the type of clock used to measure it.

At the same time, STE-QUEST searches for a possible violation of the gravitational time dilation. Such a violation may be described phenomenologically by a dependence of one or more the fundamental constants on the gravitational potential, $X = X(U/c^2)$, where X is a generic dimensionless fundamental constant or a dimensionless combination of fundamental constants. Such a dependence is a violation of the principle of Local Position Invariance (LPI), which states that the outcome of local, non-gravitational experiments is independent of where and when in the universe they are performed. If a constant depends on the gravitational potential, then the results of laboratory-type experiments, which usually depend on that constant, will also depend on the location, namely the distance from the mass distribution generating the potential.

LPI is one of the three cornerstones of the Einstein Equivalence Principle (EEP), the others being the Weak Equivalence Principle and Local Lorentz Invariance. The EEP is generally believed not to be absolutely valid, and thus worldwide experiments are undertaken to search for violations of each cornerstone.

The STE-QUEST mission is thus a probe of possible space-dependence of fundamental constants. Spatial dependence and time dependence of fundamental constants have become a very intense research topic in the last decade. The search may help to point the way toward a unified theory of all forces, reveal hypothetical extra dimensions in our Universe or the existence of many sub-Universes with different physics, chemistry and biology. Indeed, unified theories of all forces, applied to cosmology, suggest space and time dependence of the coupling constants. Another argument for spatial variation of fundamental constants comes from the anthropic principle. There must be a fine tuning of fundamental constants which allows humans and any life to appear. Life in its present form is not consistent with fundamental constants whose values only slightly differ from the actual ones. This fine tuning can be naturally explained by the spatial variation of the fundamental constants: we appeared in the area of the Universe where the values of the fundamental constants are consistent with our existence.

In the Standard Model there are three fundamental dimensionless parameters determining the structure and energy levels of stable matter (atoms, molecules): the electromagnetic fine structure constant α and the ratio of a fundamental mass (electron mass m_e or light quark mass m_q) to the strong QCD energy scale Λ_{QCD} , $X_{e,q} = m_{e,q} / \Lambda_{\text{QCD}}$. The fundamental masses m_e and m_q are proportional to the vacuum Higgs field which determines the electroweak unification scale. Therefore, the constants $m_{e,q} / \Lambda_{\text{QCD}}$ can also be viewed as the ratio of the weak energy scale to the strong energy scale.

Extensive studies of atomic and molecular spectra of gas clouds in the distant universe are currently undertaken to search for a difference of these parameters compared to today's values (see e.g. recent works [FTK] and [Fla07] for other references). Also, some differences in Big Bang nucleosynthesis data and calculations can be naturally explained by a variation of fundamental constants [Den04].

How can a space-time variation of the fundamental constants and a dependence on the gravitational potential may occur? Light scalar fields very naturally appear in modern cosmological models, affecting the Standard Model parameters α and $m_{e,q} / \Lambda_{\text{QCD}}$. One of these scalar fields is the famous "dark energy"

which causes accelerated expansion of the Universe. Another hypothetical scalar field is the dilaton, which appears in string theories together with the graviton. Cosmological variation of these scalar fields should occur because of drastic changes of matter composition of the Universe. During the Big Bang nucleosynthesis the Universe was dominated by radiation, then by cold dark matter and now by dark energy. Changes of the cosmic scalar field $\varphi_0(t)$ lead to the variation of the fundamental constants $X(\varphi_0)$. Massive bodies (Galaxies, stars, planets) can also affect physical constants. They have large scalar charge S proportional to the number of particles $S = s_p Z + s_e Z + s_n N$, where Z is the number of the protons and electrons and N is the number of the neutrons; s_p , s_e , s_n are the scalar charges of protons, electrons and neutrons, respectively. There is also a contribution of the nuclear binding energy (scalar charge of virtual mesons mediating nuclear forces).

The scalar charge produces a Coulomb-like scalar field $\varphi_s = S/R$. The total scalar field is $\varphi = \varphi_0 + \varphi_s$, therefore we may have variation of the fundamental constants inversely proportional to the distance from massive bodies,

$$X(\varphi) = X(\varphi_0 + \varphi_s) = X(\varphi_0) + \delta X(R),$$

$$\delta X(R) = (dX/d\varphi) S/R,$$

where a nonzero δX violates LPI.

The gravitational potential U is essentially proportional to the number of baryons $Z + N$ and inversely proportional to the distance, $U = -GM/R$. Therefore, the change of the fundamental constants near massive bodies can be written:

$$\delta X/X = K_{X,i} \delta (U/c^2), \quad (2)$$

where the index i refers to a particular composition of the mass M , and where the coefficients

$K_{X,i} = - (dX/d\varphi) S_i/GM_i$ are not universal, but are expected to be different for, e.g., the Sun and Earth, $K_X(\text{Earth}) \neq K_X(\text{Sun})$. Indeed, the Sun consists mostly of hydrogen; therefore the Sun's scalar charge is $S_{\text{Sun}} \approx Z(s_p + s_e)$. The Earth contains heavier elements where the number of neutrons exceeds the number of protons, $N \approx 1.1 Z$. Therefore, the scalar charge of the Earth $S_{\text{Earth}} \approx Z(1.1 s_n + s_p + s_e)$ and is sensitive to the neutron scalar charge (also, to the contribution of the nuclear binding), in contrast to the sun.

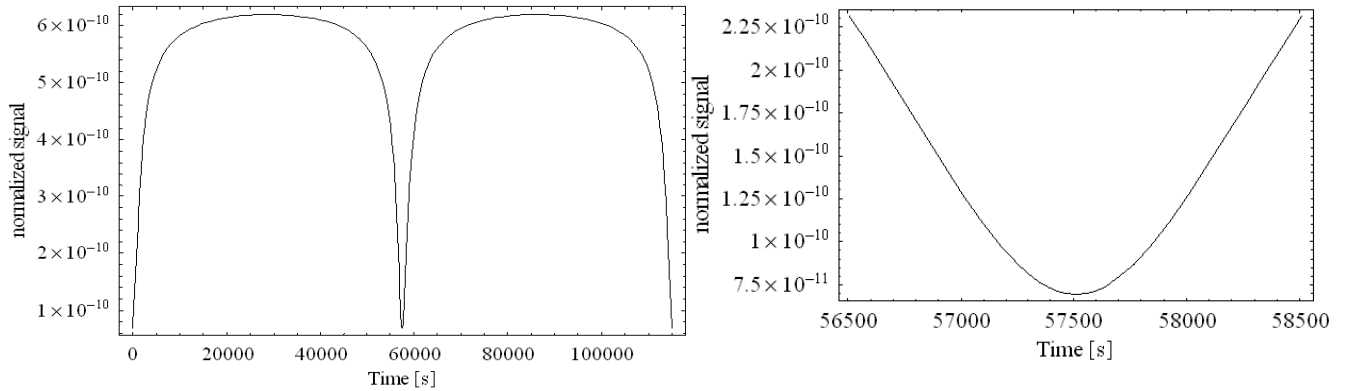


Figure C1: Gravitational potential difference $U(r_{\text{STE}}) - U(r_{\text{ground}})/c^2$ (normalized redshift signal) between satellite location and surface of the Earth, during the orbit of the STE-QUEST satellite. The time span is two orbital periods. The plot on right shows the gravitational potential difference near perigee.

The proposed STE-QUEST satellite experiments allows to set limits to $K(\text{Earth})$ and $K(\text{Sun})$, setting limits on the dependence of the fundamental constants on the neutron scalar charge s_n .

In summary, when the frequencies of two identical clocks (of nominal frequency ν_0) at different locations are compared (time dilation measurement), the result is

$$\nu(x')/\nu(x) = 1 + [1 + \sum_X A_X K_{X,i}] (U_i(x') - U_i(x)) / c^2. \quad (3)$$

The sensitivity factor $A_X = X (d \ln \nu_0 / d X)$ states the sensitivity of the clock frequency to a particular constant X , and can be calculated using atomic and nuclear theory (see e.g. [Fla07]).

The result of the STE-QUEST mission may be given as a limit for (or nonzero values of) $K_X(\text{Earth})$, with X being a (known) combination the three fundamental constants α , m_e/Λ_{QCD} , and m_q/Λ_{QCD} in case of use of the microwave clock, and α in case of the optical clock. The ground clock comparisons (null solar gravitational shift) will give limits to $K_X(\text{Sun})$ for X being α and m_e/Λ_{QCD} , respectively, using optical atomic and molecular clocks.

C.1.2 Measurement approach for the gravitational redshift

The gravitational potential experienced by the ground and satellite clocks includes the contributions from the earth and the sun (the contribution from the moon is an order smaller and may be neglected for

the purposes of the discussion, but will be taken into account in data analysis). Figure C1 shows the Earth gravitational potential at the satellite during its orbit.

The Sun's contribution to the relative gravitational potential difference is approx. 4×10^{-12} , but cancels with Doppler shifts due to the motion of Earth and of the satellite on Earth's orbit [Hof61].

Nonzero and null gravitational frequency shift signals can be measured as follows.

(1) Absolute comparison between ground and satellite clocks with the satellite at apogee

This measurement approach relies on the accuracy of the ground and satellite clocks. The difference in gravitational potential between Earth surface and apogee is $\Delta U/c^2 = 6.2 \cdot 10^{-10}$ (Figure C1). The space clock frequency at apogee is measured with respect to a ground clock. With a space clock having an accuracy of 1×10^{-16} , the redshift measurement accuracy is **1.6×10^{-7}** , **45** times better than the goal accuracy for the ACES mission. This is achieved mainly through the more appropriate orbit of a dedicated satellite compared to the low altitude ISS orbit and in part thanks to an improved performance of PHARAO when modified to operate with Rubidium atoms instead of Caesium atoms.

This measurement does not take advantage of the repetitive nature of the orbit (a single apogee measurement would in principle suffice), but will be repeated hundreds of times under different conditions, e.g. under the seasonal variation of the velocity of the Earth with respect to the stars. The solar gravitational contribution cancels, as mentioned above, due to the fact that satellite and Earth are in free-fall with respect to the Sun [Hof61]. The redshift test is performed by comparing the clock frequency shift with the value expected from gravitational potential difference. In doing so, the gravitational potential uncertainty at the location of the ground clock must be sufficiently small. It may indeed be reduced sufficiently by appropriate local gravity measurements at and above the ground clock site.

An optical clock with goal inaccuracy of 5×10^{-17} represents a realistic advanced instrument compared to PHARAO. This would improve the redshift measurement accuracy by a further factor of 2, i.e. **90-fold compared to ACES**. An additional advantage of an optical clock is the ability to determine the performance of the space clock flight model at full goal performance level *while it is still on the ground*, which is not possible with PHARAO, whose full performance relies on the presence of microgravity. Also, the characterization of the performance of an optical clock during the mission will also be significantly enhanced due to its intrinsically much higher stability and the availability of a correspondingly sensitive link, the laser coherent link.

(2) Repeated measurements of satellite clock frequency variation between apogee and perigee

This measurement approach relies on the stability rather than accuracy of the ground and satellite clocks and is complementary to (1). The ratio of ground and satellite clock frequencies is measured every time the satellite is at perigee and when it is at apogee. The difference between the two values is averaged over N orbits. Systematic shifts (if not correlated with orbital motion) are expected to average out, leading to a gain in sensitivity of up to $N^{1/2}$. This mode uses the stability properties of the satellite clock on the timescale from perigee to apogee, rather than its accuracy. For the PHARAO-MOLO clock specification of $3 \times 10^{-14} \tau^{-1/2}$, the signal-to-noise ratio (SNR) for the measurement of the redshift is approx. 1.2×10^5 per orbit, estimated using Wiener theory. For $N \sim 1000$ orbits (1.8 years, if uninterrupted), the sensitivity of the measurement improves to **2.7×10^{-7}** (**~ 27** times larger than for ACES), and thus comparable to the expected result from the absolute comparison, (1) above.

With an optical clock (advanced STE-QUEST scenario), with a stability specification $1.5 \times 10^{-15} \tau^{-1/2}$ and a flicker floor at 2×10^{-17} , the SNR is improved by a factor 15 compared to PHARAO-MOLO, to 1.8×10^6 per orbit, leading to a redshift measurement inaccuracy of **1.8×10^{-8}** (**~ 400** times better than for ACES).

In (1) and (2), the redshift is from Earth's gravitational potential. The contribution from the solar potential is strongly reduced due to the fact that satellite and Earth are an interacting system in free-fall toward the sun [Hof61].

(3) Comparisons between terrestrial clocks

The frequency comparison link between STE-QUEST satellite and ground also allows terrestrial clock comparisons by a common-view (or nearly-common-view) method, whereby the frequency signals from two distant ground clocks are sent to the satellite and compared there. It is expected that ground clocks will have reached an accuracy at the level of 1×10^{-18} and beyond at the time of the mission in 2022, a factor 9 beyond current state-of-the-art (note that the improvement of clock accuracy over the last decade has been a factor 200). The microwave link on STE-QUEST allows a comparison of the ground clocks at with this resolution within 12 days, while the more sensitive optical link achieves this within a few hours.

The measured frequency difference between two ground clocks is given, after correcting for Doppler shifts of the relative motion between ground clocks and satellite, by the difference in Earth gravitational potential at the two clock locations. The terrestrial contribution is nearly constant in time, with small seasonal variations due to e.g. the change in water table level under the ground clocks. The solar contribution varies according to the orientation of the ground clock pair with respect to the sun, i.e. with a 1 day-period, with a peak-to-peak amplitude of 8×10^{-13} . However, it is cancelled by the Doppler shifts of the motion of the ground clocks relative to each other as they orbit the Sun [Hof61]. Nevertheless, the measurement of this “null” effect is of importance. Repeated clock comparisons over the course of the mission ($N = 500$, implying approx. 1000 days using the links proposed below) will allow measuring the null solar gravitational shift up to an accuracy of 6×10^{-8} . As the Doppler shifts responsible for the cancellation can be calculated (based on independent experimental confirmation of the validity of Lorentz transformations) with at least the same accuracy, from the null result the actual Solar redshift can be deduced to the above accuracy. In comparison, the best current (pre-ACES) results for the solar gravitational frequency shift are at the few % - level [Lop91,Kri93]. The improvement compared to the ACES mission is about a factor **20**, due to the higher ground clock performance by the time of the STE-QUEST mission and the more performant optical link of STE-QUEST compared to MWL on ACES.

It is assumed that the ground clock systematic shifts with daily period average out over the duration of the large number of orbits, and that the Earth potential variations on the daily timescale can be modelled at the appropriate level.

The links of STE-QUEST are such that they can contact any location on a large fraction of the Earth's surface. Thus, global ground clock frequency comparisons at the level of 10^{-18} and less, more than two orders of magnitude below the current GPS and two-way -satellite -time and frequency transfer (TWSTFT) methods become possible. For the time and frequency community, the availability of such a global high performance microwave and optical link will accelerate the process leading to a redefinition of the SI second based on clocks operating in the optical domain.

The actually detected gravitational shift mentioned above is the quantity of interest for geophysics applications. The measurement accuracy enables Earth potential difference determinations down to a level of 1 cm equivalent height. The importance of this is not only the high sensitivity, but also the extremely high spatial definition of such measurements (the potential is measured at the location of the clock), to be compared with the relatively low spatial resolution of conventional satellite gravimetry (tens of km).

Search for neutron scalar charge

As described above, the measurements will allow setting limits to the neutron scalar charge.

C.1.3 Theoretical analysis of frequency comparison signals

The determination of the gravitational frequency shift via ground-satellite clock comparisons is complex (Eq.(1) is strongly simplified) and requires an accurate treatment of all relevant relativistic effects. Gravitation in the solar system is described in the barycentric (BCRS) and geocentric (GCRS) non-rotating celestial reference systems by means of post-newtonian solutions of Einstein's equations for the metric tensor in harmonic gauges codified in the conventions IAU2000 [Sof03]. In these conventions the relativistic structure of Newton (order $1/c^2$) and gravitomagnetic (order $1/c^3$) potentials are given. For the Newton potential the multipolar expansion of the geopotential determined by gravity mapping is used. The post-newtonian effects of the metric (described in terms of the β and γ PPN parameters) can be included. Orbits of satellites is evaluated in the GCRS at the level of a few cm by means of the Einstein-Infeld-Hoffmann equations at the order $1/c^2$ [Moy03] using the relativistic Newton potential. Instead the trajectories of the ground clocks in the GCRS are evaluated from their positions fixed on the Earth crust (ITRS, International Terrestrial Reference System) by using the non-relativistic IERS2003 conventions [IER03].

For the propagation of light rays (here: radio signals) between the satellite and the ground stations one uses the null geodesics of the post-Newtonian solution in the GCRS. The time/frequency transfer properties have been theoretically evaluated for an axisymmetric rotating body [Bla00,Lin02] at the order $1/c^4$ (i.e. with Newton and gravitomagnetic potentials developed in multipolar expansions). These results have been developed for use in the ACES mission.

The available theory is fairly complete for the data analysis in mode (2), described below. For modes (1, 3), the theory will be generalized to include the effect of the gravitational potential at the location of the ground clock(s) (including time-varying effects, such as the tides) and of the solar and lunar potentials.

The uncertainties of the various contributions above are minimized by a using precise STE-QUEST orbit data obtained by satellite tracking, and by using current and future accurate Earth gravity information. Required orbit position knowledge is at 1 cm level near perigee, and ~ 50 cm near apogee (see also [Duc09]), reachable already today with the proposed orbitography approach described below. The

validity of the special-relativistic Doppler shift (time dilation) has been and will continue to be independently verified with increased accuracy by spectroscopy of relativistic atomic ion beams at the GSI Darmstadt storage rings. Potential violations of this aspect of Lorentz Invariance are expected to be sufficiently bounded so as not to affect the signal interpretation.

C.2 Test of the Universality of Free Fall and search for new physics

C.2.1 Scientific motivation

Einstein generalised the Equivalence Principle and made it the foundation of his theory of General Relativity. A violation of Einstein's Equivalence Principle at some level would either require a modification of General Relativity or constitute the discovery of a new force. Concerning the free fall of matter, the following problems motivate a precision test.

Test of GR/metric theories: The Einstein Equivalence Principle (EEP), consisting of the (i) Universality of Free Fall, (ii) the Universality of the Gravitational Redshift and Local Position Invariance, and (iii) Local Lorentz Invariance, implies that gravity is described by a pseudo-Riemannian metric [Wil93], it thus makes definite statements on the structure of the theory of gravity, Therefore, is very important to test the EEP as fully and accurately as possible. Furthermore, the incompatibility of General Relativity and Quantum Theory implies that there has to be a new theory, called Quantum Gravity, which then necessarily has to violate basic principles underlying General Relativity or current Quantum Theory. Therefore, any test of the EEP also contributes to the search for a Quantum Gravity theory. Since there is yet no final theory of Quantum Gravity any experimental information (either restricting ranges of parameters or even finding a signal of non-standard physics) is of fundamental importance.

Anomalous spin coupling to space-time curvature: Within the formalism of General Relativity spinning test particles no longer move on geodesics but instead, according to the Mathisson-Papapetrou-Dixon formalism, experience a force consisting of the spin-curvature coupling (e.g., Dixon 1967) (analogous to the coupling of the magnetic moment to the gradient of a magnetic field yielding a force acting on a moving magnetic moment) which also can be derived from the Dirac equation in curved space-time. Any other coupling of the spin to the gravitational field would indicate a violation of the universal coupling of gravity to matter (minimal coupling) and, thus, would lead to new physics. Most prominent in this respect is the Moody-Wilczek approach (1984) where one assumes additional spin-spin, spin-mass, and mass-mass interactions.

Dilaton scenario: All string theory models predict the existence of the dilaton as a scalar partner of the graviton [Dam02]. The experimental discovery of the dilaton would provide strong evidence for string theory [Kap00]. At tree level, the dilaton is massless and has gravitational-strength couplings to matter which violates the EEP [Dam02]. Several models exist to reach consistence with experimental bounds, but there are still residual EEP violations predicted. [Dam02] suggests several mechanisms for a EEP violation around 10^{-12} including variations of fundamental constants. Improving the sensitivity of EEP tests can help to improve the bounds on several dilaton models as well as distinguishing between those models.

Space-time fluctuations: Fluctuations in the geometry of space and time are a generally expected feature of any quantum theory of gravity. The most simple model of such fluctuations are stochastic fluctuations in the space-time metric. It has been shown [Gök08] that such fluctuations lead to an apparent violation of the Universality of Free Fall for quantum systems. This violation is more pronounced for small systems thus giving an argument favouring that the Universality of Free Fall on the quantum level might be different than on the classical level. For a random walk scenario the violation would be of the order 10^{-12} , for a holographic noise scenario the violation is expected to be at the 10^{-15} level.

Standard Model Extension: Within the Standard Model Extension (SME) all possible modifications of Lagrangians including gravity are discussed. These modifications lead to violations of all aspects of the Einstein Equivalence Principle. Since the SME is a phenomenological model inspired by a symmetry breaking scenario within string theory no definite predictions can be made.

C.2.2 Timeline in context of other existing or planned facilities

Current status

There is a long history of testing the universality of free fall with macroscopic bodies, which continuously improved the measurements. Historically, there have been four distinct methods of testing the Equivalence Principle: (i) Galileo's free-fall method, (ii) Newton's pendulum method, (iii) Newton's celestial method (based on observations of the Earth-Moon system or of the moons of Jupiter in the Sun's field), (iv) Eötvös' torsion-balance method. The most precise tests today have achieved an

accuracy of 1 part in 10^{13} . They are based on modern torsion pendulum experiments, which probe the gravitational attraction of Titanium and Beryllium to the earth, the sun and dark matter. A similar accuracy is achieved by Lunar Laser Ranging which compares the free fall of the earth and the moon towards the sun.

Planned space tests with macroscopic test masses

Experiments on the ground are limited because of the limited driving acceleration and the unavoidable and unshieldable microseismicity in Earth-based laboratories. In space, experiments could be done more precisely by a factor 10^3 to 10^5 .

The first test in space will be the CNES-led MICROSCOPE project (MICRO-Satellite à Trainée Compensée pour l'Observation du Principe d'Équivalence), a room-temperature test of the Weak Equivalence Principle to 1 part in 10^{15} with classical bodies [MIC]. The drag-compensated satellite will be in a Sun-synchronous polar orbit at 700 km altitude, with a payload consisting of two differential accelerometers, one with elements made of the same material (platinum rhodium alloy), and another with elements made of different materials (platinum rhodium alloy and titanium alloy). Differential displacements between the test masses of a pair are measured by capacitive sensors for over one year. The launch is scheduled for 2011.

Another, known as Satellite Test of the Equivalence Principle (STEP), is under consideration as a possible joint effort of NASA and the European Space Agency (ESA), with the goal of a 10^{-17} test. STEP would improve upon MICROSCOPE by using cryogenic techniques to reduce thermal noise, among other effects. At present, STEP (along with a number of variants, called MiniSTEP and QuickSTEP) has not been approved by any agency beyond the level of basic design studies or supporting research and development.

Quantum tests of the equivalence principle

Quantum tests of the equivalence principle investigate the propagation of matter waves in a gravitational field. Gravity acts on matter waves similar like a material with an inhomogeneous index of refraction on light waves, which bends the straight trajectories of light waves to parabolas. According to the Schrödinger equation the bending should not depend on the nature of the matter waves. The centre of mass of packets of matter waves are expected to follow the trajectory of classical bodies, while they disperse in width. In this respect, classical mechanics can be seen as the limit of geometrical optics of quantum waves.

The phase induced by accelerations is measured by atom-interferometric methods. Atomic interferometers represent a novel technology of quantum devices for ultra-precise sensing and monitoring of accelerations and rotations. These atomic inertial quantum sensors function similar like atomic clocks, which revolutionised frequency metrology and today are the most accurate standard for time and frequency measurement. Like atomic clocks, inertial and rotational sensors using atom interferometers display a high potential for replacing classic state-of-the-art sensors. The recent improvement of the sensor performance is mainly due to the rapid progress in the laser development and in the manipulation of atoms.

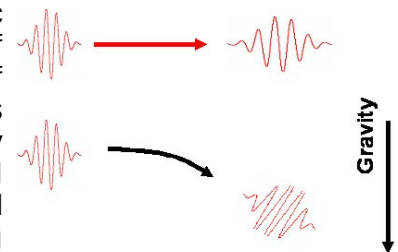


Figure C2: Schematic of a matter waves under gravity.

The potential of matter wave sensors has been demonstrated by laboratory prototypes more than 10 years ago. A high sensitivity of atom interferometers has been demonstrated by the measurement of g , the local acceleration due to gravity, with a precision of about 10^{-9} by the group of S. Chu [Pet99]. A comparison with a Michelson gravimeter based on falling corner cubes, (FG-5 produced by Micro-g-Solutions, Arvada, Colorado) with a quoted relative uncertainty of 2 ppb showed a difference of 7 ± 7 ppb due to the uncertainty of the gravity gradient measurement of 5 ppb. The resolution of the atom interferometer has been about four times higher than the FG-5 due to the higher repetition rate, the noise behaviour was similar. Limitation were the measurement time and, thus, the large gravitational acceleration.

Another very promising variant of atomic interferometer was the gravity gradiometer developed by the group of M. Kasevich. This sensor measures the gradient of gravity Δg with a precision approaching state-of-the-art mobile gravity-gradient sensors [Sna98]. This experiment is very similar to the gravity meter of S. Chu using two atomic interferometers which are roughly displaced by 1 m. However, instead of using two independent atomic interferometers the remarkable precision and robustness of this configuration is mainly achieved by using one Raman laser system for both interferometers at the same time.

Since these pioneering experiments, these sensors have been further developed for special applications and transportable sensors. Most prominent examples are the atomic sensors developed by

M. Kasevich at Stanford university or the gravi-gradiometer at the JPL by Nan Yu in the US as well as current developments at the SYRTE (PARIS), the LENS (Florence), Leibniz Universität Hannover and Humboldt Universität zu Berlin. These activities comprise sensors to measure the Newtonian constant, terrestrial gravity and the Earth rotation rate.

The first test of the universality of free fall based on comparing the free fall of matter waves of two different isotopes was recently published [Fray, *Space Sci Rev* (2009) 148: 225–232]. The measurement was based on an atom interferometer employing the two isotopes of rubidium, ^{85}Rb and ^{87}Rb . The measurement yielded a difference $\Delta g/g = (1.2 \pm 1.7) \times 10^{-7}$, which is – within the experimental accuracy – in agreement with a free fall of matter waves that is independent from internal composition. However, since in this experiment the interferometer can only be run with either ^{85}Rb or ^{87}Rb at the one time. In contrast, a test of the EP in a dual-species atom interferometer is expected to yield a large gain in sensitivity from cancellation of systematic effects.

C.2.3 Measurement approach to the Universality of Free Fall

The proposed mission will compare the free evolution of two species of atomic wavepackets via interferometric means and thus provide a test of the universality of free fall in the quantum regime.

The most suitable interferometer type for measurements of gravity is the Mach-Zehnder type, due to its high symmetry. In a Mach-Zehnder interferometer atomic wave packets made out of cold atoms are coherently split, re-directed and re-combined to observe matter wave interferences. Beam splitting is achieved by the atom-light interaction.

Beam splitting is achieved by the atom-light interaction. During each interaction sequence the atoms are exposed to a pulsed light field generated by two counter-propagating laser beams. An atom absorbs a photon out of one laser beam and is stimulated by the other laser beam to re-emit the photon. In this way twice the recoil of a photon is transferred coherently to the atomic wave (rather than atoms) to generate a new spatial mode of a matter wave. For a Mach-Zehnder-type atom interferometer the phase shift due to accelerations a can be calculated by the following formula:

$$\Delta\phi = \mathbf{a} \cdot \mathbf{k}_{\text{eff}} T^2 = \mathbf{a} \cdot \mathbf{k}_{\text{eff}} L^2 / v_{\text{at}}^2$$

The equation is derived from the Schrödinger equation and describes the gravitational phase shift of matter waves in a Mach-Zehnder type atom interferometer. The equation has important implications: The phase shift depends only on the acceleration, the momentum difference of the two interfering matter waves and the square of the drift time of the matter waves inside the interferometer. This simplicity recommends atom interferometer as inertial references for measuring absolute accelerations. The momentum difference of the two interfering spatial matter wave modes is determined by the photon recoil of the light beam interacting with the matter wave, a well defined quantity. The equation states also the equality of the inertial and the gravitational mass as it is independent of the atomic mass of the particular species.

Figure C3 shows a schematic of the atomic interferometer employed by STE-QUEST. It is sensitive only to one axis for accelerations. The schematic illustrates the time sequence of the laser pulses. The centre of mass motion of the atomic ensemble is zero before entering the interferometer. Ensembles of two different species are prepared at the same time and interact coherently with laser pulses matched to both species

The sensitivity of the atomic accelerometer increases for a given length scale L of the detection volume and effective photon recoil k_{eff} of the interferometer with the square of the atomic drift time T or the inverse square of the atomic velocity. Thus, for an atomic accelerometer the sensitivity as well as the precision by using ultra-cold atoms in a space-bound experiment would increase by several orders (10^3 to 10^4) of magnitude allowing longer measurement times.

Two benefits of microgravity help in achieving these longer interrogation times. The sample does not fall out of the interrogation area as in for ground-based setups limited to tens of milliseconds. The spread of the cloud can be kept sufficiently low by utilizing BEC with a sharp momentum distribution prepared in low frequency traps. This is difficult on ground since in typical trap configurations low trap frequencies are associated with shallow traps which cannot compensate for gravity.

The preparation and observation of such samples in a microgravity environment has been

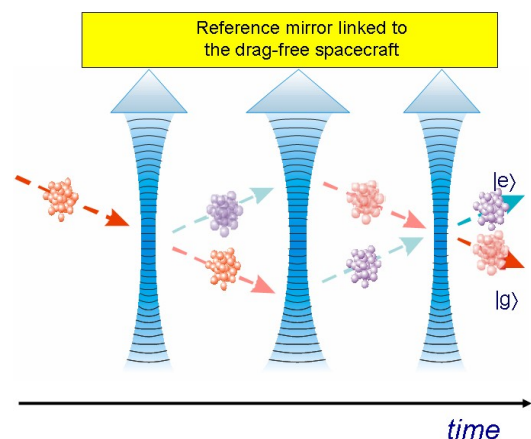


Figure C3: Schematic of a Mach-Zehnder matter wave interferometer.

demonstrated recently for expansion times of up to 1s [Zoe10].

For comparing the free fall of matter waves of two rubidium isotopes, QUEST will synchronously operate *two* atom interferometers. This means that preparation of the matter wave packets by laser cooling and trapping as well as their coherent manipulation during the interferometer cycle is done at the same time. For signal separation, the detection of the interferometer output after the interferometer cycle will be done successively in a narrow time window of a few milliseconds. The synchronous operation guarantees a suppression of common mode accelerations with respect to the satellite, which was demonstrated on ground-based experiments up to 140 dB. The use of two isotopes of rubidium facilitates the synchronous operation and automatically guarantees alignment of the two interferometers as the laser light for manipulation for cooling, detection and coherent manipulation can be delivered in one fibre.

STE-QUEST will make pair wise comparisons between the two isotopes of rubidium while it orbits around the earth. For one comparison, the targeted sensitivity of one part in 10^{15} will be reached for a total integration time of about 1 month. Since the measurement will only take place during periods of low altitude and respectively high local gravitational acceleration this takes about 2 years of mission time. Most of the needed calibration of the system can be done during high altitude phases of the orbit. This should allow for exceeding the targeted accuracy in a 5 year mission.

C.3 Local Lorentz Invariance tests

There has been an explosion of interest in Local Lorentz Invariance in recent years [SR], with numerous astronomical studies and many new high-precision experiments applied to search for violations of Lorentz Invariance. Significant developments have also occurred on the theoretical side, and a theory (standard model extension, SME) has been worked out that provides a unified framework for discussing Lorentz Invariance violations. Two aspects of Lorentz Invariance can be tested with STE:

Independence of the speed of light from the laboratory velocity

A possible dependence of the speed of light on the speed v of the laboratory, can be described, according to the Mansouri-Sexl (MS) test theory, by

$$c(v) = c_0 (1 + B v^2/c^2)$$

Here $v = 377$ km/s is the velocity with respect to the cosmic microwave background, the cosmologically preferred frame, and B is a combination of parameters describing deviations from the usual Lorentz transformation formulas.

The rotation of the Earth around its axis modulates v with a ± 300 m/s amplitude. This can be used to search for a time-dependent frequency difference between an optical cavity, whose frequency is proportional to c , and an atomic reference, e.g. the optical clock. The advantage of a space experiment is the high orbital velocity and strongly reduced deformation due to microgravity [Läm01]. For the proposed elliptic orbit, v varies between $+4$ km/s and -4 km/s over approx. one hour. This variation is 13 times larger than the change of the velocity of the Earth's surface, and occurs over a shorter time scale. This is advantageous, since over such relatively short intervals the drift of the cavity is more predictable. The large number of orbits permits substantial averaging. An improvement by a factor 20 compared to the best terrestrial results is expected.

During the mission, the difference between reference cavity frequency in the MOLO and a ground clock frequency is continuously monitored and is available for data analysis. This analysis will be performed in the framework of both the MS and SME theories, taking into account complementary bounds obtained with terrestrial experiments and from astrophysical observations.

Independence of Zeeman splitting frequency on the direction of the magnetic field

A class of tests of Lorentz invariance consists in measuring the frequency splitting between two levels of a quantum system induced by a static magnetic field, as a function of orientation of the field direction with respect to the stars (Hughes-Drever-type experiments). This class addresses the so-called matter sector, and is complementary to combined-photon/matter-sector tests such as the above. The SME again provides a complete framework for analyzing such experiments [Kos99]. The most precise experiments are performed with atomic clocks, e.g. masers or cold atom clocks [Wol06]. The STE-QUEST instruments allow such experiments, since magnetic fields are applied continuously in the clock or repeatedly for calibration. Compared to terrestrial experiments, the advantage of STE-QUEST is the high velocity as mentioned above, leading to an improvement by factor ~ 20 . It is noteworthy that with the optical clock, a sensitivity to the electron parameters is given, while the Cs clock signals can be used to test the proton parameters.

C.4 Spin-off to other fields

STE-QUEST will allow establishing a global reference frame for the Earth gravitational field with accuracy in the order of a few cm in terms of the geoid heights. Such a reference frame will serve as reference for all gravity field modeling and clocks will be used to define time scale (TAI) and Earth gravitational potential at the same time. With ground clocks at 10^{-18} accuracy level, a new type of geodesy will become possible, where geometry will be measured by GNSS systems and physical heights and potential by mobile optical clocks.

Following the first static gravity field models from by the CHAMP mission, the GRACE mission for the first time gave insight into the temporal variations of the gravity field [Tap04]. The best GRACE gravity field models reached a precision of about 1 cm over ~ 250 km half wavelength [Rei05]. However, for typical Earth topography with height variations of e.g. 1000 m over 30 km horizontal distance, one may expect variations in the geoid of about 80 cm. Such a high-spatial frequency signal in geoid variations cannot be detected by space gravity missions and requires a combination of satellite and terrestrial gravity measurements, like gravity anomalies, deflections of vertical and GPS/levelling points. The best combined global gravity field models are provided up to degree and order 360 in terms of spherical harmonic representation, corresponding to a half-wavelength of about 55 km. However, in combining the satellite and terrestrial gravity field measurements the problem of terrestrial data given in different height systems between continents and different countries remains and has to be tied to satellite measurements.

The geodetic scientific community is currently establishing a Global Geodetic Observing System (GGOS), [Rum00]. Its objectives are the early detection of natural hazards, the measurement of temporal changes of land, ice and ocean surfaces as well as the monitoring of mass transport processes in the Earth system. Global change processes are small and therefore difficult to quantify. Therefore the required precision, relative to the Earth's dimension is 1 ppb. GGOS will be established by the combination of geodetic space techniques (GPS, Laser-Ranging, DORIS, VLBI) and realized by a very large number of terrestrial and space-borne observatories. The purely geometric terrestrial 3D coordinate system is in good shape and fully operational. It has to be complemented, however, with a globally uniform height system of similar precision. The current precision level of regional height systems, in terms of gravity potential differences, is on the order of $1 \text{ m}^2/\text{s}^2$ (10 cm) with inconsistencies between these various systems up to several $10 \text{ m}^2/\text{s}^2$ (several meters). The actual requirement in the context of GGOS is $0.1 \text{ m}^2/\text{s}^2$ (1 cm) with the need of a permanent, i.e. dynamical, control. This requirement of high precision height control comes from the need to understand, on a global scale, processes such as sea level change, global and coastal dynamics of ocean circulation, ice melting, glacial isostatic adjustment and land subsidence as well the interaction of these processes. Only by means of monitoring in terms of gravity potential changes at the above level of precision the change of ocean level can be understood as a global phenomenon and purely geometric height changes be complemented by information about the associated density or mass changes.

The geoid can also be defined in a relativistic way [Bje85], as the surface where accurate clocks run with the same rate and where the surface is nearest to mean sea level. The relation between the differences in the clock frequencies and the gravitational potential is given in simplified form by Eq.(1). At present there is no operational way to compare frequencies of the already available optical clocks on the global scale at the same level as their accuracy would allow. With STE-QUEST and highly accurate ground optical clocks it will become possible to obtain gravitational potential differences on a global scale by comparing frequencies. This comparison will have both an extremely high spatial resolution (the size of the atomic ensemble, less than 1 mm) and a high temporal resolution (as high as 0.5 days). This would be a significant new dimension to gravity field determination, since such observables are given on the global scale and provide in situ local gravity information at the same time. STE-QUEST will allow clock-based gravitational potential mapping with strongly enhanced performance compared to ACES.

D Mission profile proposed to achieve these objectives

D.1 Launcher requirements

The CDF Assessment Study of the STE concept with a highly elliptic orbit and a spacecraft wet mass of 1048 kg has evaluated the appropriate launcher requirements. As for this proposed STE-QUEST mission the orbit is the same while payload mass increases by 50 kg or 107 kg (advanced STE-QUEST scenario) we do not expect any changes of the launcher requirement.

The baseline launch profile assumes 3 Fregat burns while additional burn might be required to correct for the optimal injection parameters.

Launcher	Sojus-Fregat
Launcher performance	> 1600 kg allowable

Launch site	CSG (Kourou) or Baikonur
-------------	--------------------------

D.2 Orbit requirements

The orbit must satisfy two main requirements:

- (I) Large gravitational potential difference between apogee and perigee
- (II) Long contact time to at least one ground stations at perigee
- (III) Simultaneous visibility of satellite from distant continental observation stations for several hours.

To satisfy the primary objective, the orbit must be highly elliptic. The perigee should be low. A very low perigee means a short contact time, which decreases the accuracy of the frequency measurement. In the ESA CDF study on the STE-QUEST mission, the following scenario has been chosen:

Period:	16 hours:
SMA:	32203.7 km
Eccentricity:	0.7802
Apogee Altitude:	~51000 km
Perigee Altitude:	~700 km
Inclination:	63.43 deg, argument of perigee: 342 deg
RAAN	0 deg, True Anomaly: 0 deg
Repeat pattern:	48 hours (3 orbits)
Maximum eclipse duration	3 hours

Within one year, the season with eclipses up to 3 hours are not more than 20 days while most of the days the duration of the eclipse is not more than 30 minutes. Within this orbit, the spacecraft has to cross the van-Allen radiation belts twice per orbit, which results in a quiet harsh radiation environment. The crossing of these belts requires hard components or an enhanced shielding. The thermal control of the spacecraft is of course more demanding than in an sun-synchronous orbit, since there are much longer eclipse times. To maintain this orbit, a Δv is required to stabilize it, which is reached with an active 3-axis stabilization of the spacecraft.

Launch is from Kourou. The maintenance of this orbit requires a $\Delta v=28$ m/s per year on average. Figure D1 shows the ground track of this orbit.

This orbit yields $\Delta U/c^2 = 5.5 \times 10^{-10}$ between perigee and apogee (Fig. C1) or 79% of the theoretical maximum between the Earth's surface and infinity. Fig. C1 shows that in the range of 1000 s around perigee the gravitation potential already changes by 10% relative to the overall amplitude. Thus, the measurement time available to determine the largest gravitational potential is only a small fraction of the orbit period.

Three ground stations on different continents have good visibility of the STE-QUEST satellite near perigee. The ground stations have been chosen as Boulder (Colorado, USA), Tokyo (Japan) and a central European city (e.g. Munich), as these

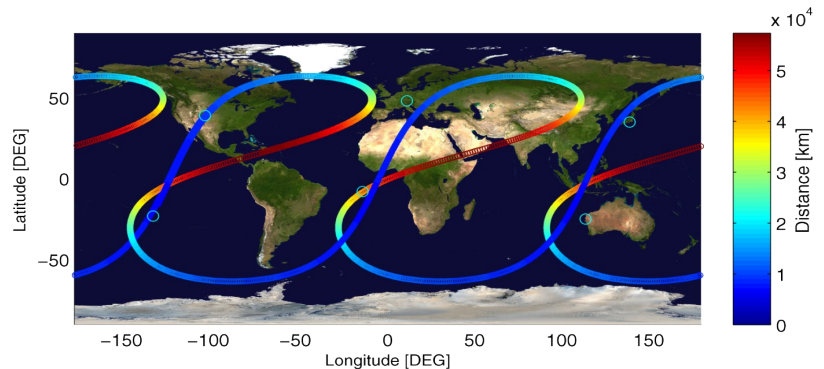


Figure D1: Ground track of STE-QUEST orbit (from CDF study). "Distance" is the height above ground. The circles show the location of the considered ground stations. Minimum for the mission goals are just two ground stations in the northern hemisphere.

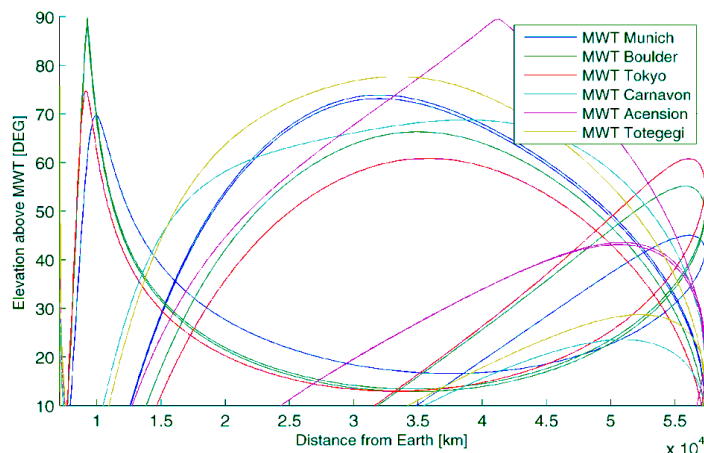


Figure D2: Elevation angle for different ground stations (from CDF study). The last three ground stations in the legend are located in the southern hemisphere. "Distance from Earth" means "distance from Earth center". "MWT" means "microwave terminal". 10 degree above the horizon was taken as cutoff.

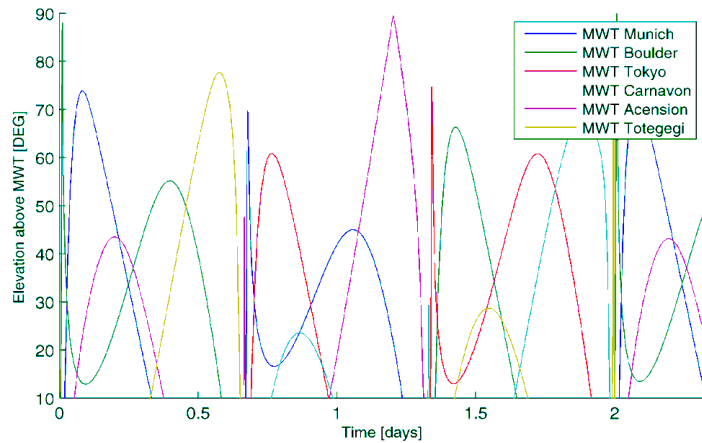
are locations where optical clocks exist today or will likely exist at the time of the mission, and where optical/microwave link stations can be set up.

The elevation of STE-QUEST as seen from the various ground stations are shown in Fig. D2.

Moreover, these stations have good visibility of a large fraction of the orbit, including continuous visibility between perigee and the following apogee.

Finally, the visibility of STE-QUEST from different ground stations, and therefore the common-view visibility from continents, necessary for the null solar gravitational redshift measurement, is shown in Fig. D3.

Figure D3: Elevation angle for different ground stations as a function of time. This plot shows the times at which two ground stations are able to contact simultaneously the STE-QUEST satellite (from STE CDF study).



As can be seen, the view of the STE-QUEST satellite by a given ground station repeats after 2 days. The common-view visibility between the selected northern hemisphere ground stations is approximately 6 hours. Common-view visibility is also possible between facultative southern hemisphere stations and northern hemisphere ones. This means that the relativistic geodesy can be performed over all continents, provided that ground stations are set up there. Of course, the common-view visibility of STE-QUEST is also given between additional stations on a single continent.

D.3 Mission lifetime

The STE-QUEST mission is designed for a nominal lifetime of up to 5 years.

D.4 Communication requirements

The data transfer rate will be 288 Mbyte/orbit (approx. 40 kbps on average) for the microwave clock and 150 kByte/orbit for the atom interferometer. For the housekeeping data, a rough estimation of 5 kbps or 36 MByte/orbit is assumed. The overall data rate is then about 45 kbps or 324 Mbyte per orbit. Data will be stored on board (2 Gbyte capacity) and transferred to earth once a day to a receiving station.

D.5 Ground segment requirements

The mission requires two separate ground segments: the science ground segment and the standard satellite TM/TC.

D.5.1 Science ground segment

A sufficient number of ground stations for achieving the goals in fundamental physics is 2, located in the northern hemisphere, on distinct continents. Three candidate stations are shown in the above Figures.

The microwave link allows performing comparisons also under conditions of cloudy sky, so it is robust. The laser link, whose use is advantageous for the common-view comparisons, requires clear weather. With ground station locations selected for simplicity (i.e. where there already today is a frequency metrology infrastructure or a laser ranging ground station), clear weather will be available only part of the time. Estimating to 25% the time fraction of clear weather at both ground stations, would reduce the measurement sensitivity of the primary goal II by a factor 2. Thus, the availability of additional or alternative ground stations would be desirable. This is realistic since (i) it is expected that by the time of the mission several laboratories will possess ultra-high performance clocks, especially in Europe, (ii) in Europe the development of long-distance high-performance fiber-optic links is in progress. These will allow separating the optical receiver/transmitter station from the clock location. This further simplifies and reduces the cost of increasing the time that clear weather conditions are achieved for common-view comparisons. Finally, container-based transportable ground stations (clock + link) operated at locations with particularly good weather conditions are also a realistic possibility.

The spin-off science results on relativistic geodesy require a larger number of ground stations, e.g. mobile ones, both on the northern and southern hemisphere. We believe that such stations are realistically possible, procured e.g. at the national level.

The communication requirements for atom interferometer are rather low, since no direct link between

satellite and ground station is needed for operation and data can be stored onboard and downloaded once per orbit.

D.5.2 Ground station equipments

Each ground station is ideally equipped both with a MWL terminal and an optical terminal plus a high performance optical clock ($< 1 \times 10^{-15}/\tau^{1/2}$ instability, 1×10^{-18} inaccuracy). As described above, the latter must not be exactly at the location of the terminals, but could be distant by a few 100 km, linked by a terrestrial fiber-optic, stabilized link.

Microwave link (MWL)

MWL uses dedicated small transportable terminals, which can be easily installed at any location of interest. The terminal interfaces to ground clocks by either electrical link at distance up to 15 m or by fiber optical link at larger distance. Two interfaces are provided: 100 MHz for conventional clocks and 10 GHz for high performance clocks. The interface to an optical clock is via an optical frequency comb, which is a standard device usually available at any optical clock.

A network of at least 2 ground terminals is assumed, having optical clocks or linked to optical clocks via optical fiber link. One ground terminal with access to UTC will transfer UTC to the S/C, thus synchronising the whole MWL network to UTC.

The system is fully compatible to ground terminals installed for the ACES mission. The availability of those will increase the number of users. The station's operation is automatic and unattended. Schedule and orbital data are received via LAN once per day. S/C signal acquisition is fully autonomous. Data are available after each pass. The terminal has an uplink data channel of 1 kBit/s and a downlink data capacity of up to 10 kBits/s. For the local user, there is a visual interface, providing quick-look data from real-time comparison to the S/C clock to verify its good health. The final full performance product is calculated at the science data centre.

The MWL terminals are modified compared to the ACES ground terminals by having a larger antenna (1 - 2 m) and increased transmit power (5-10 W) to account for the higher S/C altitude. The main bi-directional link operates in Ka-band. Compared to ACES, the highly elliptic orbit will considerably reduce link-induced systematic errors due to slower variations of the link geometry. STE-QUEST user access is significantly enhanced, providing significantly longer observation times, a larger on-ground coverage area and due to a nearly arbitrary high number of simultaneous on-board receiver channels.

Technology heritage: The MWL ground terminal electronics is similar to the ACES MWL ground terminal, except for the Ka-band technology, which is from the STE-QUEST flight hardware. The design of the ACES MWL ground terminal is shown in Figure D3. (MWL GT, Figure D3)

TRL: 9. Proposed procurement: ASTRIUM, TIMETECH, TZR, and EREMS

Optical link

The ground segment for the optical link (OL) will consist of two or more (e.g. 3 to ensure permanent coverage) laser tracking stations.

Present satellite and lunar laser ranging stations (organised within the International Laser Ranging Service (ILRS)) are well adapted for this purpose, but will require upgrades concerning the optical set-up (wavelength, Doppler cancellation, adaptive optics) and need to be linked to high performance ground clocks, with an attractive option being the use of optical fibre networks to transfer the performance of the best clocks from distant labs to the ground stations [Jia08]. The phase coherent detection requires adaptive optics (AO) methods to ensure phase coherence over the complete aperture. The wave-front sensor of the adaptive optics would use the incoming signal, with the necessary AO configuration and performance under study within the scope of national (CNES, DLR) or ESA activities (ITT 6404, 2010).

An alternative and/or addition to the use of existing ground stations is to develop mobile ground stations like the one developed for the LCT at DLR or the one used in [Gre10]. This is especially useful for the

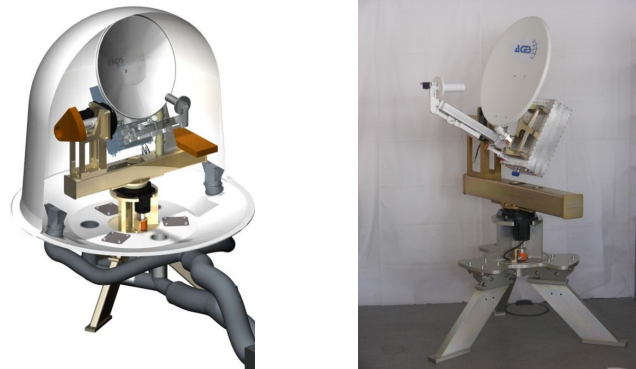


Figure D4: ACES MWL ground terminal system design (left) and in the assembly phase (right); STE-QUEST design will be similar, but with larger antenna dish

goal of mapping the geopotential. The strong turbulence conditions in low altitude urban areas might oblige one to avoid those and use astronomical observation or other selected sites (and thus either high performance clocks at those sites, or fibre links), depending on the performance of the AO systems under study. In the following we will consider as a baseline ILRS type ground stations with a “standard” 1 m aperture telescope. The error sources for the optical link have been analyzed, and it was found that the dominant contribution is atmospheric turbulence [Dje10], limiting the the stability to about $\sigma_y(\tau) \approx 5 \times 10^{-15}/\tau$ (Figure E2).

D.5.3 Satellite tracking via laser ranging

Laser ranging is alternative to MWL ranging, and also serves for absolute calibration of the latter. For this purpose an on-board corner cube reflector (CCR) is provided. Ranging will be done with the ILRS. Ideally, the satellite will be ranged at every perigee passage and every apogee passage, simultaneously with the frequency comparison procedures. Today’s ranging precision is sufficient to satisfy the science goals. For apogee observations in the northern hemisphere, a large number of stations is available. The number of stations capable of ranging at or near perigee is more than 6, and thus is sufficient, even considering unfavourable weather conditions at some of these. The MWL ground stations are able to range even under those conditions.

D.5.4 Alternative mission scenarios

A reduction of the mission duration from several years to 2 years would reduce the number of orbits over which the measurements can be averaged. This would reduce the accuracy of the tests by a factor of about 2. In addition, the shorter mission duration would reduce the number of ground clock comparisons useful for geopotential mapping, and thus the make the map coarser.

D.6 Critical issues

For the proposed approach the main critical issues are related to the payload TRL and require some further developments described below.

In the current concept the spacecraft bus has been chosen based on the Proteus line to rely on heritage as much as possible. The equipment and avionics system however can not be used as is on the Proteus bus but equipment from geostationary spacecraft is proposed. This ensures also sufficient TRL for the spacecraft subsystems.

E Proposed model payload to achieve the science objectives

E.1 Overview of all proposed payload elements

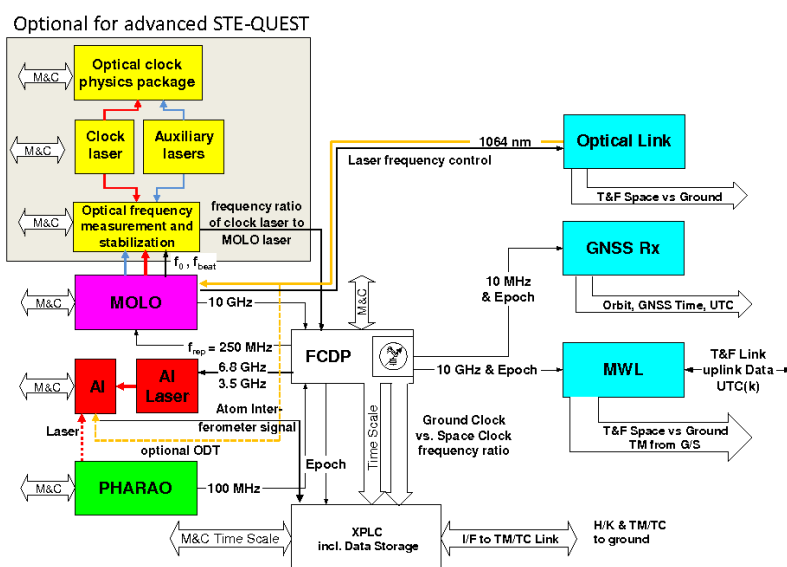


Figure E1: Schematic of the payload units and their signals. The schematic shows both the baseline STE-QUEST payload (PHARAO is the clock) and the advanced version (PHARAO is replaced by the optical clock in the grey shaded box).

The science goals require clocks of as high as possible frequency stability on the timescale of half the orbital period (6 h) as well as on the time scale of perigee passage (~ 1000 s). Only clocks based on cold atoms are suited for the science goals (Fig. E2). We consider two scenarios.

In the first, the TRL-8 cold atom clock PHARAO is used, where its performance is improved by a factor ~ 3 by using an optically derived microwave signal generator (MOLO).

The satellite payload consists of a cold-atom clock (baseline scenario: PHARAO; advanced scenario: optical clock), a dual species atom interferometer, an optical-microwave local oscillator (MOLO), an on-board frequency distribution unit (FCDP), two independent satellite-to-ground clock comparison units (MWL, OL), and the onboard computer/control system (XPLC), see Fig. E1. Auxiliary units are the position determination

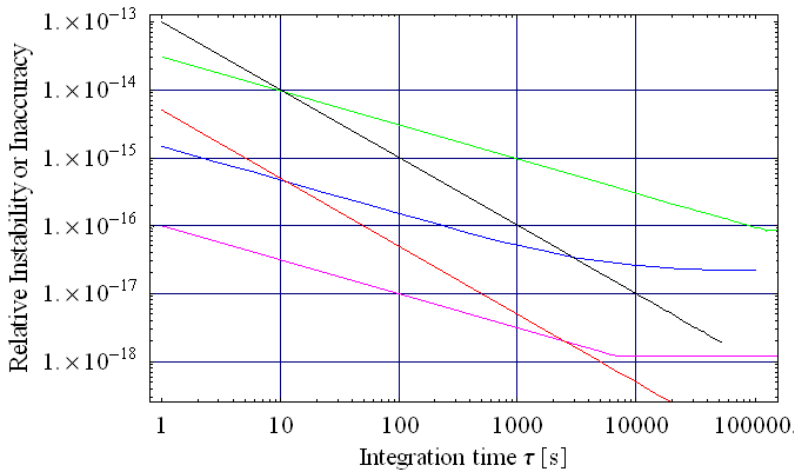


Figure E2: Performance of clocks and links on STE. **Black:** microwave link and optical link in near-common-view ground-ground comparison mode; **green:** PHARAO clock incl. MOLO; **red:** optical link for space to ground comparisons; **blue:** optical clock (STE-QUEST advanced scenario); **pink:** projected ground optical clock performance in 2022. For the proposed orbit, the integration time is limited to approx. 6 hours for (near-) common-view comparisons of ground clocks on different continents, while the comparison of a single ground clock with the satellite clock is possible for up to 14 h.

GPS/Galileo receiver (GNSS), attitude monitor (star tracker, not shown), and the CCR (not shown).

In the advanced STE-QUEST scenario, PHARAO is replaced by an optical clock package. The package contains the atomics package (atom generation and trapping), the auxiliary lasers for atom cooling and manipulation. The clock laser for the optical clock is also in the package, but without a corresponding reference cavity. Instead, the clock laser is frequency-locked to the already present MOLO via the frequency comb contained therein. Furthermore, the auxiliary lasers in the optical clock are frequency-stabilized via the frequency comb.

The MOLO uses the Nd:YAG laser oscillator in the optical link, saving power, volume, and weight. The optical link (OL) uses a Nd:YAG laser transmitter/receiver and a telescope with active pointing. The MWL is an enhanced version of the ACES MWL,

taking advantage of a higher and ultrapure oscillation frequency of 10 GHz, derived from the MOLO.

The two links (MWL, OL) differ in their performance, see Fig. E2. The optical link is a factor ca 20 more sensitive than the MWL in case of a continuous comparison between a space and a ground clock. This means that the same measurement sensitivity can be achieved within a 20 times shorter time interval. This is particularly relevant in case that a highly stable space optical clock is used. For comparisons of ground clocks, the two links are of similar performance, allowing comparing future ground clocks at the level of their expected future accuracy (10^{-18}) within about 2 orbits. A much shorter time, 3 hours, would be sufficient, if two independent LCTs are on the spacecraft. This option would be feasible in terms of power and mass. Inclusion of both link types provides a high level of redundancy and provides independent approaches to ensure the accuracy of the clock comparisons.

The dual atom interferometer is based on concepts developed for experiments on microgravity platforms (QUANTUS). It will be able to sense minute differences in the gravitational acceleration of the individual atomic isotopes with respect to the drag-free spacecraft. The differential measurement suppresses common mode accelerations due to the residual motion of the spacecraft by more than 100 dB. The ideal type of atom interferometer for this objective is a so-called Mach-Zehnder-type, as pointed out in section C.

The many similar technological requirements between atomic clock and atom interferometer allow for significant sharing of payload components, such as the MOLO, the FCDP, the PHARAO laser system. Hence, in normal science operation STE-QUEST will toggle between clock mode and interferometer mode. The phases in which clock and interferometer alternate are chosen with respect to the different performance of the experiments during the periods of the orbital day. As the atom interferometer's sensitivity reaches its maximum in the proximity of the Earth it is operated when the satellite orbits close to the perigee. The clock on the other hand requires a large modulation in the gravitational potential and is therefore operated during most of the path from the perigee to the apogee. However, the long mission duration also offers the alternative to run only the clock for a substantial number of consecutive orbits (including perigee passages, which is especially relevant if the advanced STE-QUEST scenario with an optical clock is selected) and then change to interferometer-only operation..

E.2 Summary of each instruments key resource characteristics

E.2.1 Microwave clock

The baseline clock for STE-QUEST is a microwave clock based on ensembles of cold atoms. It is essentially based on the PHARAO clock developed by CNES in the framework of the ESA ISS mission "ACES". The ACES flight in 2014 will fully establish its performance. In STE, this clock is upgraded using the microwave-optical local oscillator and an optimized atom source and laser system and especially by using ^{87}Rb [Läm04]. This improves significantly the clock performance. The specification is

a relative instability (Root Allan Variance) of $3 \times 10^{-14} (\tau/s)^{-1/2}$, i.e. at the integration time of 10 000 s it drops to 3×10^{-16} and to 3×10^{-17} at 1 000 000 s. While this specification is a factor 20 less stringent than for the optical clock, the lower cost of obtaining a flight model and the frequency's sensitivity to the particle masses makes it a good baseline choice for STE. The accuracy of PHARAO using Rb is specified at 1×10^{-16} , with the goal of 3×10^{-17} .

Description and key characteristics The PHARAO cold atom clock is one of the two atomic clocks of the space mission ACES managed by ESA. PHARAO is a caesium clock based on laser cooled atoms and has been developed by SYRTE, LKB, and CNES (France). It is proposed here to include a second version of this instrument, modified to work with Rubidium instead of Caesium, as its cost/performance ratio is very attractive for the STE-QUEST scientific objectives. The PHARAO concept is very similar to ground based atomic fountains, but with the major difference of zero-g operation. Atoms slowly launched in free flight cross two microwave fields tuned to the transition between the two hyperfine levels of the caesium ground state (Figure E3). The interrogation method, based on two separate oscillating fields (Ramsey scheme), allows the detection of an atomic line whose width is inversely proportional to the transit time between the two microwave cavities. The resonant microwave field at 9.192631770 GHz (SI definition of the second) is synthesized starting from an ultrastable quartz oscillator (USO). For Rb, this frequency will be changed to 6.8346826109 GHz.

The clock has 3 operating modes: The quartz oscillator can be a flywheel oscillator or phaselocked to an external oscillator (here, the MOLO), or frequency locked to the clock line. In the nominal operating mode the intrinsic qualities of the caesium hyperfine transition, both in terms of accuracy and frequency stability, are transferred to the quartz oscillator or to the external oscillator. In a microgravity environment, the velocity of atoms along the ballistic trajectories is constant and can be changed continuously over almost two orders of magnitude (5-500 cm/s). Differently from atomic fountain clocks presently operated on ground, very long interaction times (up to few seconds) will be possible, while keeping reasonable the size of the instrument.



Figure E3: The PHARAO engineering model (EM under test).

The physical package of the clock has 4 main sub-systems. A laser source provides the laser beams required to cool, select and detect the caesium atoms, a frequency chain generates the microwave signals. They are connected to a vacuum chamber where the caesium atoms are manipulated. The caesium tube consists in a UHV chamber pumped by getters and a 3 liter/s ion pump, a caesium reservoir, a microwave cavity, coils to provide a uniform magnetic field and 3 layers of magnetic shields. Vacuum windows with fiber-optics collimators enable the transmission of the cooling and detection light onto the cesium atoms. A computer with a dedicated software drives and surveys the clock operation and processes the data communications.

The EM of PHARAO has been assembled at CNES Toulouse and fully tested. As this clock is not optimized to operate on Earth, the performances will be degraded during ground tests. The expected frequency stability would be about $4 \times 10^{-13} \tau^{-1/2}$ whereas a $10^{-13} \tau^{-1/2}$ frequency stability is expected in microgravity. In both cases the stability level is mainly defined by the quartz oscillator phase noise. The ultimate frequency stability, which is defined by the quantum noise would be $2.2 \times 10^{-13} \tau^{-1/2}$ and $5 \times 10^{-14} \tau^{-1/2}$ respectively. A further improvement is expected for the PHARAO-Rb version, which will operate with increased number of atoms.

The PHARAO-Cs frequency stability is currently $3.6 \times 10^{-13} \tau^{-1/2}$ and reaches $2.2 \times 10^{-13} \tau^{-1/2}$ when the quartz oscillator is replaced by a cryogenic oscillator. Consequently the PHARAO-Cs frequency stability will be lower than $1 \times 10^{-13} \tau^{-1/2}$ in microgravity. For PHARAO-Rb, the level will be $3 \times 10^{-14} (\tau/s)^{-1/2}$.

An evaluation of the PHARAO frequency accuracy was performed, with the goal to obtain an accuracy budget in the 10^{-15} range. The 4 main contributors were evaluated: the blackbody radiation effect, the Zeeman shift, the first order Doppler phase shift (amplified by the gravity) and the cold collision frequency shift. The total frequency uncertainty of the PHARAO clock operating on earth has been evaluated at the level of 2.1×10^{-15} . When the PHARAO clock is compared to the primary frequency standard FOM, all the measurements obtained in different configurations give a frequency difference within 2×10^{-15} . These results validate the PHARAO-Cs clock as a new space primary frequency standard with a frequency inaccuracy less than 3×10^{-16} . The flight model design is now validated.

The improvement from using ^{87}Rb comes from the much lower collision shift of the Rb than the Cs (a factor 50) as it has been demonstrated in SYRTE [Sor00] and Yale University (USA). This allows a higher number of atoms in the atomic source needed to improve the short term stability and also a

better long term stability (a factor 3), as it is the main limitation for Cs. The two other main systematic effects, cavity pulling and black body radiation shifts, are also reduced in the case of Rb. Long term stability at the 1×10^{-16} is regularly obtained in ground Rb fountain at SYRTE and will be improved in micro-gravity thanks to the longer interaction time. The higher long-term stability will directly reflect into an improvement of the measurement accuracy by at least a factor 3 compared to Cs.

Resources The overall instrument has a weight of 91 kg and a max. power consumption of 110 W.

Current heritage and TRL The technology readiness level of the PHARAO-Cs clock is 8 as most sub-systems either have already successfully passed qualification levels for ISS environment and Japan HTV launcher or are in the process of doing so. All PHARAO technologies are space qualified (including random vibrations and thermal cycling). The operating temperature range is 10-33 degrees and non operating temperatures -40 +60 degrees. The flight of PHARAO-Cs on the ISS is foreseen for 2014. This will establish its performance under microgravity conditions and will give input for improvements and modifications, if necessary.

In order to qualify the Rb version of PHARAO, the laser diodes, which operate at 780 nm instead of at 852 nm for Cs, have to be space qualified. This is a minor modification as the rest of the optical bench and payload are identical. Moreover, the Rb laser chips are very similar to the Cs ones as they belong to the same semiconductor family. They are commercial devices and widely used since more than 10 years in atomic physics laboratories. Finally, these lasers have been already tested under vacuum and in micro-gravity, in the Bremen Drop tower in the frame of the QUANTUS program of DLR. Taking the necessary qualification the laser diodes into account, the TRL level of the Rb version of PHARAO is 7.

Proposed procurement: SODERN

E.2.2 Microwave optical local oscillator (MOLO)

This oscillator is composed of three main subunits: the reference cavity, the frequency comb and the electronic lock systems (Figure E4)

Reference cavity subunit

Description and key characteristics. The reference cavity serves to stabilize the optical frequency of the Nd:YAG laser providing a laser linewidth ~ 0.4 Hz ($\sim 1 \times 10^{-15}$ relative to optical frequency) and a frequency drift < 0.1 Hz/s. The cavity is made of ULE (ultra low expansion coefficient glass) with two high-reflectivity mirrors, resulting in a cavity finesse of about 300 000. Designs of the resonator that include a stable mounting capable of withstanding shocks have been developed, e.g. spherical cavities supported at "magic" points. The symmetric support of the cavity in the three dimensions also suppresses strongly the influence of the residual vibrations of the satellite on the laser linewidth. The resonator resides inside the aluminium vacuum chamber with a 3 liter/s ion-getter pump; vacuum 10^{-8} mbar. Two stages of polished aluminium shields are implemented around the cavity, and active temperature stabilization at the exact zero crossing temperature of the ULE thermal expansion coefficient using TEC elements between the shield and the vacuum chamber. An additional active temperature stabilization of the whole vacuum chamber is also included. The optical setup for frequency stabilization will be a reflection-type lock using Pound-Drever-Hall (PDH) scheme, where an electro-optic modulator (EO) applies a phase modulation. The phase modulator is contained in the LCT. A polarizing beamsplitter and Lambda/2 plate in front of the cavity will be used to detect the reflected from the cavity signal. A double-pass acousto-optical modulator (AO) is foreseen in front of the cavity for isolation from the back reflections. Control electronics includes two temperature stabilization systems, RF driver for the AO, amplified low-noise photo-detector for the PDH lock and frequency lock electronics. Coupling of the clock laser radiation to the cavity is via single-mode polarization maintaining optical fiber. The path length noise in the fiber between the reference cavity and the laser will be actively compensated by a feedback stabilization system (not shown in the Figure E4).

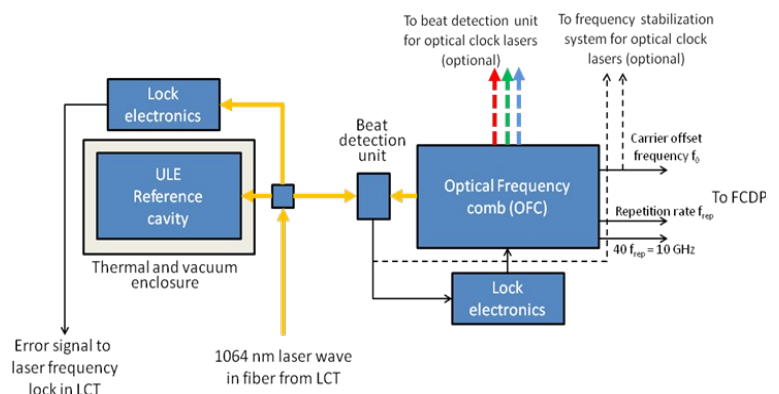


Figure E4: MOLO consisting of reference cavity, optical frequency comb, and associated electronics. The laser itself is in the laser coherent terminal. Black lines: electronic signals; coloured lines: optical waves.

Performance assessment with respect to science objectives. The performance of this unit is

enhanced by the microgravity environment, and the low residual acceleration level of the satellite ($a_{\text{rms}} < 1.10^{-6} \text{ g}$) does not limit the achievable laser stability. In the room temperature ULE cavity the frequency stability is limited by thermal $1/f$ noise in the mirrors, leading to a plateau of the Allan standard deviation below but near 1×10^{-15} for times from 1 to 20 s. This is compatible with the specified overall clock performance of the optional optical clock, and satisfies by far the requirement of the spectral purity and stability of the 10 GHz signal for PHARAO.

Resources: Including control electronics: 15 liter, 12 kg, 8 W

Current heritage and TRL. The specifications are based on standard performance on laboratory prototypes and on the successful demonstration of a transportable ULE reference cavity [Vogt 2010], see Figure E7. A simplified ULE cavity with lower finesse for the stabilization of the LCT laser has been developed and space-qualified by the company TESAT (Germany).

Very-high-reflectivity mirrors have TRL 4; their radiation resistance must be still be tested. Already space qualified elements (TRL 9) are acousto-optical modulator (CNES, ACES mission), ULE (NASA, LISA mission), optical fibre (Naval Research Laboratory), Fiber collimators (LightPath Technologies), TECs (Marlow Industries, Inc.), vacuum Pumps, temperature controllers (CNES, ACES mission).

Critical issues. A possible degradation of the high-reflection cavity mirrors under space conditions by radiation. If necessary, this will be prevented by an additional radiation shield.

Proposed procurement approach: European space industry, e.g. SODERN, ASTRIUM, Kayser-Threde

Laser subunit

The Nd:YAG laser is actually located in the LCT. It is a space-qualified Nd:YAG laser (Figure E6). This type of laser can be stabilized to a high-finesse cavity with a relative stability of better than 1×10^{-16} .

Current heritage and Technology Readiness Level (TRL). 9 (Has flown in space on TerraSAR X)

Proposed procurement approach: TESAT

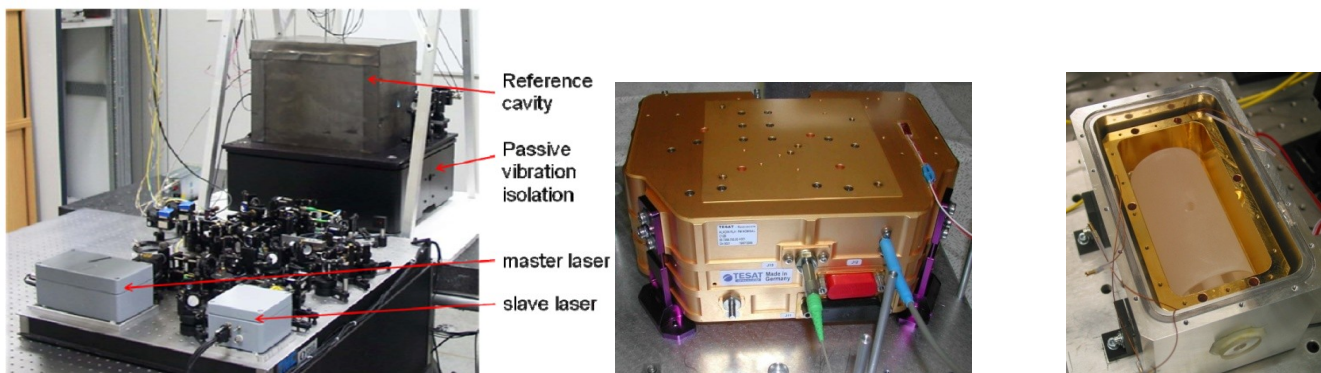


Figure E5: Left: Transportable clock laser for interrogation of a Strontium optical lattice clock (PTB Braunschweig) [Vogt 2010]. In the background is the reference cavity with its enclosure. This cavity has successfully been transported on the road over 800 km without changes in properties. Center: ALADIN LIDAR Reference Laser Head (RLH), similar to the laser for STE. Optical power: 20 mW. Physical parameters: 2 liter, 2 kg, 20 W. Right: example of a compact reference resonator vacuum chamber assembly. Top plates were removed. The inner, actively temperature-stabilized, housing is gold-coated. The ULE cavity length is 10 cm.



Figure E6: Right: Optics module of optical frequency comb for operation in the drop tower. It is based on an Erbium-doped fiber laser plus amplifiers. Right: electronics module. This fully phase-locked comb has first been dropped in March 2010 and has withstood 40 g acceleration upon termination of drop. Volume of optics module is ca. 30 liter.

Optical Frequency Comb (OFC) subunit

Description and key characteristics. A femtosecond fiber laser based optical frequency comb generator (OFC) will be used to produce a spectrally ultrapure microwave local oscillator output for the operation of PHARAO, of the microwave link and of the GPS/GALILEO receiver. The femtosecond laser is based on erbium-doped fiber, pumped by fiber-coupled laser diodes. It emits 100 fs pulses at a repetition rate of 250 MHz, with an average power of 100 mW. The emission spectrum is centered around 1560 nm. Spectral broadening to more than one octave is obtained via nonlinear interaction in a microstructure fibre, so that the range from about 1050 nm to 2100 nm is covered. Second harmonic generation of a portion of the broadened spectrum allows to obtain carrier envelope frequency f_0 .

Specifications: Generation of an ultrapure 10 GHz signal using 2 mW input from the ULE-cavity-stabilized 1064 nm laser radiation. The frequency f_0 is phase-locked to (a fractional multiple of) the repetition rate and the repetition rate is controlled so that the beat signal with the 1064 nm laser is a fraction of the repetition rate itself. Alternatively this beat could be phase-locked to a USO-derived radiofrequency signal. The directly detected 40th harmonic of the repetition rate of 250 MHz is the desired 10 GHz output for the FCDP. The status of the locks is monitored. The specification for the Allan deviation of the derived 10 GHz signal is a flicker floor 3×10^{-15} from 0.1 to 10 s.

Performance assessment with respect to science objectives It has been demonstrated by several groups that the commercial frequency comb from MENLO systems satisfies the above specifications. The performance of a rocket-proof comb will be established by 2013 in a DLR project.

Resources: Projections for a space qualified OFC, based on industrial terrestrial technology and drop tower prototype, foresee a total weight of 16 kg, volume of 20 l and 38 W power consumption. Of this, the optics package is envisaged by Menlo Systems to use 3 liter and 10 W of power. These values are for a comb suitable for PHARAO. For STE-advanced with the optical clock, the additional beat unit is 2 l, 2 kg, 1 W.

Current heritage and TRL. Commercial frequency combs are routinely used in many laboratories world wide: Fiber laser OFCs are largely based on a technology that has been developed for optical telecommunication. The development of space frequency combs is under way. Initial studies were performed under ESA contract. A robust frequency comb has been recently been developed for use in the Bremen drop tower and has already undergone successful drops (see Figure E6). In a DLR development project "FOKUS" (2010-2012), a rocket OFC will be developed in 2011, vibration tests are planned for 2011, and the demonstration of the comb in a sounding rocket is planned for 2016 (no radiation resistance specification). Thus, TRL 7-8 will have been achieved by 2014.

Critical issues. The doped optical fibers are known to be susceptible to degradation through ionizing radiation. It has been shown in the framework of the above project "FOKUS" that two solutions are possible: fibers can be designed so as not to be susceptible or they can be bleached or annealed so as to remove the color centers produced by the ionizing radiation.

Proposed procurement approach: MENLO Systems

E.2.3 Atom interferometer

Description and key characteristics

The atom interferometer is a dual species apparatus based on the two isotopes of rubidium, ^{85}Rb and ^{87}Rb . It is measuring the differential acceleration of two atomic isotopes along one axis. For achieving an optimal suppression of common-mode-noise, which accords to basically all possible disturbance sources, the two atomic species are simultaneously prepared, coherently manipulated and detected with optimally overlapped atomic clouds of the two species. The device consists of a vacuum chamber with an integrated atomic source and a magnetic shielding. As key parameters have been a number of atoms of 10^6 a free evolution time between beamsplitter pulses $T = 5$ s with a resulting repetition rate: 1/11s. With this parameters the single shot precision will be 2.48×10^{-12} , the target sensitivity at the 10^{-15} level will be reached after an integration over 635 days or 950.

Performance assessment with respect to the science objectives

Testing the universality of free fall at a level of one part in 10^{15} implies a measurement of accelerations with the atom interferometer to a similar level of precision. By multiplying with the gravitational acceleration at the satellites position the sensitivity in m/s^2 can be calculated, which is the applicable unit for atomic accelerometers. As g decreases with distance also the acceleration in m/s^2 has to be determined to a more precise level. For estimating the overall sensitivity we consider the g value at the highest altitude used for the interferometer mode (3000 km over ground). Hence the calculated value is a very conservative estimation for the actual sensitivity.

Following the formula $\varphi = \mathbf{a} \cdot \mathbf{k} \cdot T^2$, one can assess the sensitivity accelerations by the resolution of the

interferometers phase shift ϕ and the scaling factor $k \cdot T^2$ of the interferometer. The resolution of the interferometers phase shift is ultimately limited by the shot-noise of the splitted atomic waves, which is given by $N^{-1/2}$, with N the number of atoms contributing to the interferometer signal. With 10^6 detected atoms, a drift of 10 second and a transferred momentum given by the wavelength λ of the 2-photon Raman transition with $\lambda = 2\pi \cdot k$ we expect a single shot accelerational sensitivity of $2.48 \cdot 10^{-12} \text{ m/s}^2$. Integration of the measured accelerations during 1000 orbits will therefore lead to an accelerational sensitivity of $3.07 \cdot 10^{-15} \text{ m/s}^2$, including a typical preparation time of 1 second before each interferometer measurement. This corresponds to a test of Einstein's Equivalence Principle of one part in 10^{15} within two years. The condition can be even more relaxed when different data sets of the five year measurement can be combined.

The limitations of this setup are determined primarily by effects which affect the two atomic isotopes in a different way. The experimental configuration rules out several of such problems. The centres of mass of both atomic clouds coincide due to the symmetric expansion, even though the velocities of both atomic species might slightly differ.

In a dual interferometer operated in the same place spatial and time variations of gravity drop out of the differential signal. This allows for a high accuracy without the need for an exact knowledge of height or angle of measurement.

As a result a spatial variation like the gravity gradient only enters during the time the atomic ensembles are separated due to their different recoil velocity during the beam splitting process.

The resulting differential signal is given by the change in position by the relative acceleration. For a $^{85}\text{Rb}/^{87}\text{Rb}$ interferometer with an interrogation time of 5 s operated at an altitude of 1000 km and taking a linear gradient into account, this effect leads to a Offset of $3 \cdot 10^{-17} \text{ m/s}^2$. This is strictly below our targeted accuracy.

An excellent common-mode rejection can also be achieved for noise sources, such as the phase noise caused by the beam splitters (using the same quartz oscillator for the two microwave synthesizers needed for the beam splitter lasers), the noise due to aliasing (since both atomic isotopes interact at exactly the same time with their respective beam splitter laser), the vibrational and rotational noise (by using the same optical elements for both beam splitter lasers).

The ultimate limitations are possibly due to interactions between the atoms themselves and the distinct light shifts sensed by the atoms when they interact with the beam-splitting lasers. The light shifts, however, can be possibly measured using in addition a microwave clock. These lightshifts cancel at a certain intensity ratio and detuning of the counterpropagating raman laserbeams. Therefore they can be neglected providing a sufficient control of the detuning and the intensity ratio.

Ultra-cold atom source

The baseline scenario of QUEST assumes that the source for generating ultra cold atoms is not implemented within the microwave clock. Currently two approaches are studied for generating atomic ensembles close to quantum degeneracy (Bose-Einstein condensation)

Atom chips provide a very compact and robust setup for harsh environments as shown in [Zoe10]. The manipulation of atoms relies on magnetic fields provided by the atom chip. The here shown second generation atom chip setup is designed to provide higher atom numbers and a shorter loading time of the atom chip. With this atom chip setup the loading of a BEC of 10^6 atoms in less than 2 seconds will be possible. It is currently under investigation in drop tower experiments and for a rocket campaign at the end 2013. The shown scientific setup fits in a volume of 0.08m^3 . The second generation of the chip shown in the picture to the right can be assigned TRL 4 and will be tested in a relevant environment in 2011.

Optical dipole traps (ODT) using high intensity far off-resonant light offer an interesting alternative route for the fast and compact production of Bose-Einstein condensates (BEC) [Bar01]. Exposing atoms to an ODT, e.g.

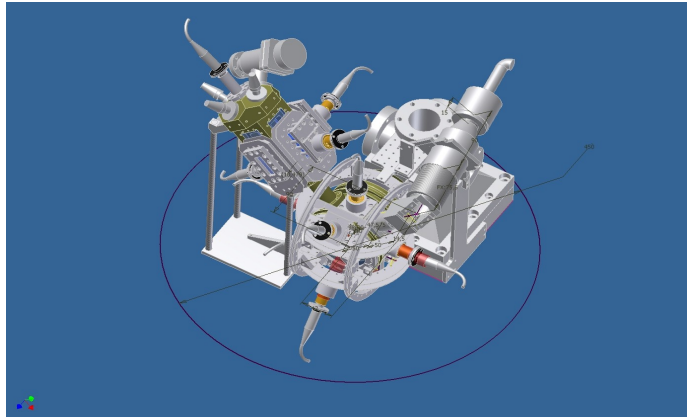


Figure E7: CAD model of the QUANTUS II double MOT system.

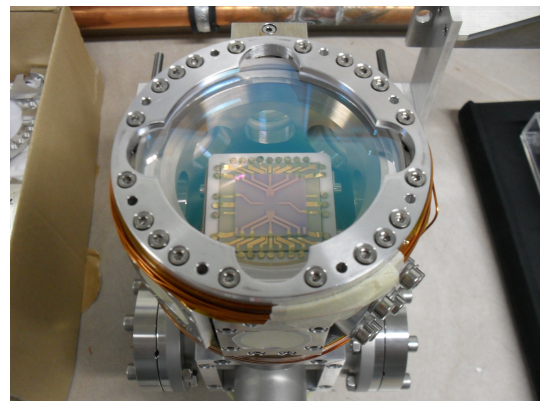


Figure E8: The QUANTUS II chip already mounted in the vacuum chamber

created by a focussed CO₂-laser beam, causes the atoms to be subject to a position dependent AC-Stark shift. Use of ODTs allows for the construction of benign traps eligible for evaporative cooling and thus the production of BEC within a few seconds or less. Evaporative cooling is typically achieved by dynamically decreasing the ODT laser intensity. Hence the hottest atoms of the atomic ensemble are able to escape the trap. In recent publications several schemes allowing for runaway evaporation in optical traps have been demonstrated [Cle09] [Jun08].

Opposed to the use of an atom chip the implementation of an ODT does not require the presence of surfaces close to the atomic ensemble, thus avoiding wavefront errors and forces occurring close to surfaces. Nevertheless the ODT approach requires the mission to carry a space suitable (radiation resistance etc.) fiber laser to create the intense laser radiation necessary for ODT operation. Also, the current technology readiness level for fiber laser in space for quantum optical applications is most likely not reached yet, thus making further research and development essential in this field.

The most promising approaches on generating rubidium atoms in dipole traps were demonstrated at a wavelength of 1.55 μm and 1.9 μm in the laboratory. The 1.55 μm laser has already been tested in parabolic flights and should reach TRL5 by end of 2014.

In order to take advantage of the long expansion times made possible with the satellite facility, we need atomic sources expanding over reasonable distances after 10s. A key method to this aim is the use of very shallow initial traps to release the atomic sample from. This was demonstrated with chip devices and led to very long observation times [Zoe10]. In the Fig. E9 we illustrate the possibility to use a BEC source of Rb atoms and have it in a spatial range where it can be observed after 10s. The spatial expansion is simulated using the well-known scaling approach of references [Cas96] and [Kag96].

It is worth noticing that a thermal source of atoms is impossible to use and this even for extremely shallow traps of frequencies as low as few Hz. In fact, the cloud is expanding very quickly and in order to be able to observe it after 10s one needs to have very cold samples (of the order of 1nK temperature). In this regime it is impossible to avoid seeing a considerable fraction of the atoms condensing.

Procurement approach: Atomic Source: Leibniz Universität Hannover, Institut Optique Atomique; Theory & Modelisation: SYRTE, ZARM, Universität Ulm

E.2.4 Laser bench

The laser system for the AI will be composed of two parts. One is the PHARAO laser system, which can also be used for the AI. The second is specific for the AI. For it, the Ferdinand-Braun-Institut (FBH) will develop free-space coupled, micro-integrated diode laser modules for laser cooling and atom interferometry of Rubidium (780 nm). For a single species the following micro-integrated laser modules will be deployed:

An ECDL-master laser with integrated Rb spectroscopy unit. This module will provide the optical frequency reference for Rb with an accuracy of better than 300 kHz.

Two ECDL-master laser power amplifiers (MOPAs), that are based on an ECDL master laser and a tapered amplifier. Each module will provide 1 W of optical output with a short term (10 μs) linewidth below 100 kHz. Two modules are used for the Raman beam and cooling light generation. One module will be offset locked to the master laser and the second module will phase locked at 3.5/6.8 GHz (Rb) to the first one.

FBH has developed a technology platform ("micro-bench"

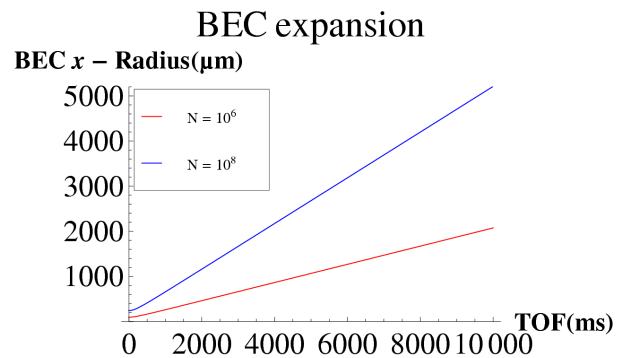


Figure E9: Spatial extension of two BECs of 10^6 and 10^8 atoms. These BECs are prepared in traps of frequencies $w_x = w_y = 0.5 \text{ } 2\pi \text{ Hz}$ and $w_z = 1 \text{ } 2\pi \text{ Hz}$. The respective chemical potentials and critical temperatures are $\mu_1=0.48 \text{ nK}$, $\mu_2= 3.05 \text{ nK}$ and $T_{c1}= 2.8 \text{ nK}$, $T_{c2}= 13.2 \text{ nK}$. It is clear that even after 10s the BEC width in the x-direction is in a region of about 1 cm where it can still be observed.

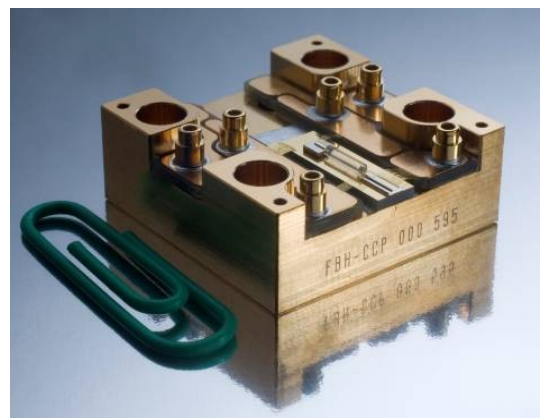


Figure E10: DFB-MOPA integrated within a $25 \times 25 \times 10 \text{ mm}^3$ volume with micro-bench technology. The front end of the conductively cooled package shows the ceramic microbench with the DFB laser coupled to the power amplifier by means of a micro-optical gradient index (GRIN) lens, FBH.

technology) which provides the means to micro-integrate semiconductor-chips, micro-optics, and electronics on a ceramic body. Using this technology, very recently the generation of more than 1 W of optical power near 1060 nm with a FWHM linewidth of approximately 100 kHz (10 μ s) and an intrinsic linewidth of 3.6 kHz could be demonstrated. The electrical power consumption by the semiconductor components, a DBR master laser and a tapered power amplifier, was less than 4 W. FBH has developed micro-integrated extended cavity diode lasers that are required when lasers have to be phase locked as for Raman beam generation in atom interferometers or as local oscillators in optical clock applications.

The development will be based on the results of research activities that are currently carried out at FBH within projects funded by the DLR (Deutsches Luft- und Raumfahrtzentrum) and the EU FP7. The development currently ongoing aims at reaching TRL 5.

Procurement approach: Ferdinand-Braun-Institut, Humboldt Universität zu Berlin

E.2.5 Frequency comparison and distribution module

Description and key characteristics FCDP accepts an ultra-stable and ultra-clean reference frequency in the 10 GHz range from MOLO. It generates several coherent reference frequencies for other payload elements by integer frequency division, including those for MWL (1 GHz, 100 MHz), MOLO (250 MHz), LCT-Modulation (125 MHz) and GNSS Rx (10, 20 MHz). It locks the Pharao-internal USO to the reference using a digital PLL. A small quartz oscillator is synchronised to this reference, which acts as continuously available on-board time scale providing epoch pulses (1pps, 1000ps) and numerical date & time information to payload elements, including the XPLC. The on-board time scale is synchronised to UTC at start-up using the GNSS Rx or MWL. Thereafter, it is continuously compared to UTC, using the same instruments. The phase noise of the reference signal from MOLO is measured against the high purity signal of the PHARAO USO for routine MOLO performance assessment. In case of contingency, FCDP synthesises the payload reference signals from either the Pharao-USO or from the USO inside the MWL. Optional for advanced STE-QUEST, it accepts and measures the frequency ratio of clock laser to MOLO laser. A fixed frequency offset, settable by ground tele-command in steps $<10^{-15}$, is introduced at the MOLO reference input to bring it close to the nominal 10 GHz target frequency. This cancels any small frequency offset up to ± 2 MHz arising from MOLO operation and allows accurate synchronisation of the on-board time scale to UTC.

Performance assessment with respect to science objectives The FCDP distributes the full performance reference from the MOLO directly to LCT and MWL, with negligible deterioration of the available signal performance. Its intrinsic stability (ADEV) is $<10^{-14}/\tau$. The nominal onboard frequency offset can be set in steps of $<10^{-15}$.

Resources: 8 kg, 7 liter, 12 W, TC:10 kByte / day, 50 kByte / day (FCDP alone)

Operating modes: The nominal mode is "Locked to MOLO". In case of contingency, the modes "Locked to PHARAO" and "Locked to MWL-USO" are available.

Current heritage and TRL: The proposed STE-FCDP reuses modules and highly stable synthesiser technology developed for the ACES MWL and ACES FCDP. The embedded Instrument Controller is dual redundant. It is implemented in radiation tolerant (100kRad) FPGA. TRL is 8.

Proposed procurement approach: TIMETECH

E.2.6 Microwave link (MWL)

Description and key characteristics

In the ESA CDF Study a scenario for the STE MWL was discussed. It differs somewhat from the estimates we have produced below. However, this difference is not critical.

The microwave link (MWL) is a two-way, i.e. bi-directional, triple-frequency link between space and ground. Its primary function is accurate frequency comparison and time transfer between space and ground clocks. The bi-directional architecture compensates to highest extent the propagation path delay and its variations arising from the S/C position and relative motion. The slant range to ground terminals is measured at cm level supporting orbit determination. Satellite laser ranging (SLR) is used to calibrate the ranging measurements.

Two bi-directional microwave links are in Ka- and Ku- band and third down-link channel is in S-band, with pseudo-noise (PN) coding. The Ka-band link is of highest performance, the S-band link supports ionospheric correction. The Ku-band link is optionally foreseen to retain compatibility to eventually available ACES-MWL ground terminals. MWL uses a combination of carrier phase and code phase measurements, representing phase- and group velocity respectively, to determine the total ionospheric delay and its variations with high stability and precision. This method compensates ionospheric effects

to any order while using a single Ka-band signal. S-band resolves carrier cycle ambiguity in Ka-band and provides differential Doppler data specific for each ground terminal. Key modulation parameters are: Ka band: Dual-PN, Tone 250 MHz, PN: 20 MChip/s; Ku band: PN 100 MChip/s; S-band: 5 Mchip/s. MWL uses the ACES MWL architecture electronics to a large extent, with minor, low risk changes: Ka-band is the primary link instead of Ku-band. Two antennae per band instead of one adapt to the large signal dynamics, with switch-over at times of low scientific relevance. The S-band link is in a primary frequency allocation, Ka-band frequencies are in the planned primary frequency allocations at 22 /26 GHz.

The change to Ka-band increases the link precision and its stability. Using a 10 GHz reference input allows significant simplifications by use of integer number frequency dividers and multipliers, which results in superior carrier frequency stability compared the ACES MWL. The ACES MWL synthesis chain was optimised to meet ACES mission requirements with minimum complexity and risk, but it exhibits well known limitations by flicker noise, which are eliminated by the proposed design.. The Ka-band receiver architecture is mixed analogue digital with all-digital control loops, which becomes feasible by use of a dual-PN (pseudo-noise) coded signal with a rather low signalling rate of 20 MChip/s instead of 100 MChip/s. The digital implementation allows reception of multiple simultaneous signals from up to 10 ground stations. The dual PN concept exhibits higher link stability compared to a single PN signal of equivalent bandwidth. This high performance is feasible for this application, while ACES MWL signal characteristics had been constrained by operation onboard the ISS.

MWL implements two different antennae for perigee and for apogee per band, with the following specs:
S/C Antenna 1 (for Perigee): 8 dBi, beamwidth = 100°
S/C Antenna 2: (for Apogee): 20 dBi, beamwidth = 14°; incident power is 1..3 W for each downlink.

Performance assessment with respect to science objectives

The planned changes on board and on ground will make the STE-QUEST MWL link compatible to STE-QUEST science and mission requirements with the following key parameters:

End-to-end link fractional frequency stability (ADEV), including ground: $\sigma_y(t) < 1.6 \cdot 10^{-13}/t$, $1s \leq t \leq 10000s$

Ranging uncertainty: 1 cm

Resources: Mass: 18 kg, Volume: 18 dm³, Power: 55W, TC: 2 kByte/d, TM: 120 MByte/d

Pointing and alignment requirements: Pointing: attitude knowledge to 1°, Alignment: none

Operating modes Continuous operation, no mode changes, regular internal delay monitoring in orbit

Calibration requirements Signal delays: 5 ns prior to launch. Ranging by SLR to 1 cm, once per year.

Current heritage and TRL TRL = 8. Microwave links have been successfully operated in space before (Gravity Probe A experiment). PRARE / ERS-2 provided cm-level geodetic-grade ranging over 12 years. The ACES MWL uses the proven PRARE concept, with a 10 times performance improvement mainly by use of modern components and higher modulation and carrier frequencies. This method is extended towards the design of the proposed MWL to meet STE-QUEST mission requirements.

Proposed procurement approach: ASTRIUM, TIMETECH

E.2.7 The optical link payload

It was found that for the science requirements of STE-QUEST an optical link with a measurement of the optical carrier phase is not necessary. Instead, timing of the code that is phase-modulated onto the optical carrier (at a comparatively low code frequency of 1 GHz) will be sufficient. This allows using the LCT terminal (TESAT, see below) with only minor modifications as it already includes a phase modulation (at GHz frequency) used for communications in the present LCT. These modifications consist in two additional interfaces that bring available signals out of the LCT. Figure E12 shows a photo

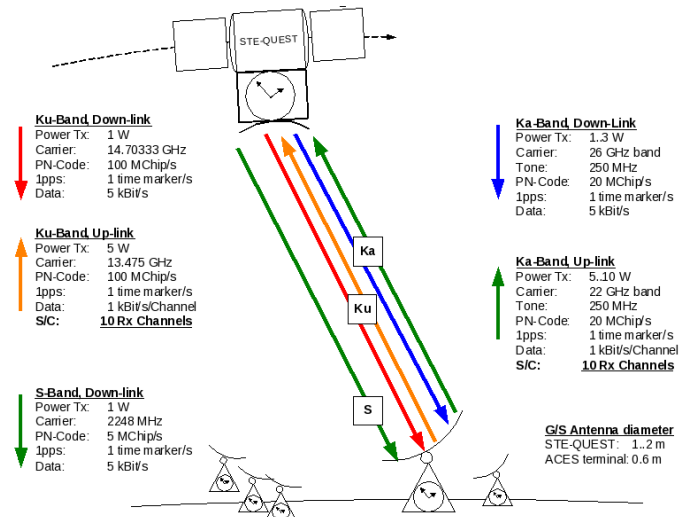


Figure E11: STE-QUEST MWL link concept and characteristics

of the LCT terminal and a schematic drawing of the OL link based on that terminal. As a relatively simple upgrade, an optical carrier phase measurement can be considered, but at the present time this is deemed unnecessary given the STE-QUEST requirements.

The high performance time transfer of OL, combined with the high performance onboard clock allows using a single LCT terminal to compare two ground clocks in view, by rapidly switching from one clock to another. This saves cost, mass and power with respect to a strict common view (which requires two LCT terminals), whilst leading to remarkable performance in the ground clock comparison.

Performance: For the satellite – ground comparison in a two way configuration the noise is dominated by atmospheric turbulence as described above and estimated in [Dje10]. The performance is then $\sigma_y(\tau) \approx 5 \times 10^{-15}/\tau$, below the performance of the onboard clock after integration times of ≈ 20 s or less.

For the comparison of two ground clocks A and B that have simultaneous visibility of STE-QUEST a “switch” comparison method is proposed, that uses a single onboard LCT terminal and telescope that is alternately switched between the ground stations. Each cycle consists of an acquisition time (dead time

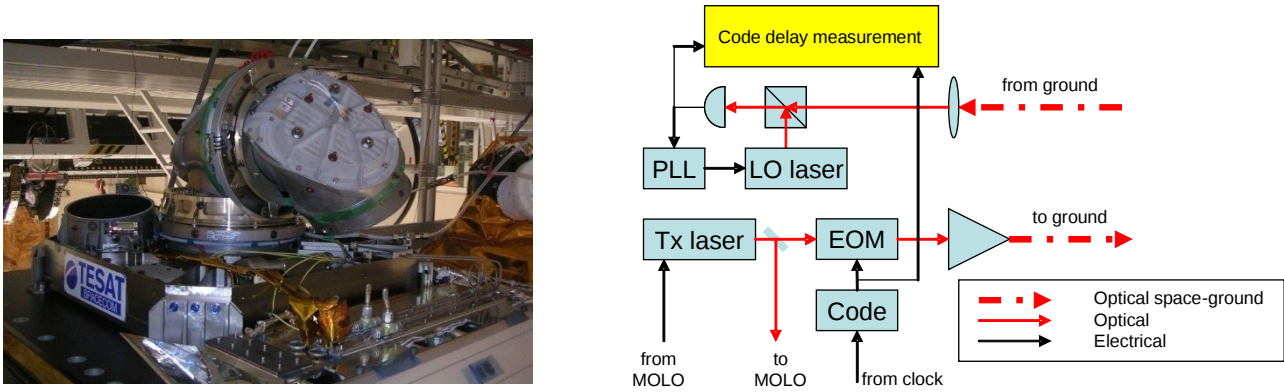


Figure E12: Optical link space segment based on LCT and block-diagram.

for the comparison) T_d with station A, a measurement time T_m for the time comparison with A, followed by an identical acquisition and measurement at B. The duration of the complete cycle is then $T_c = 2(T_d + T_m)$. Based on existing experience with the LCT the acquisition time is estimated as $T_d \approx 60$ s. The measurement time T_m has to be long enough for the link noise to average below the onboard clock noise, which, with the link noise limited by atmospheric turbulence is the case after less than $T_m \approx 20$ s. Allowing for some margin this leads to a cycle time of $T_c \approx 200$ s. The phase noise on the resulting ground-ground comparison for one cycle can then be estimated as: $\sigma_{xA-xB}^2(T_c) \approx \sigma_{x-linkA}^2(T_m) + \sigma_{x-linkB}^2(T_m) + \sigma_{x-Sc}^2(T_c/2)$, where $\sigma_{x-linkX}(T_m)$ is the phase noise of the link S/C to station X averaged over the measurement time T_m and $\sigma_{x-Sc}(T_c/2)$ is the phase noise cumulated by the space-clock over half a cycle. We will assume that the link noise is white phase noise up to 20 s, but flicker phase (e.g. (de)modulation electronics noise) for longer integration times, i.e. it does not average with the number of cycles N_c . The third term averages with N_c as the cumulated phase over independent intervals T_c is uncorrelated for white frequency clock noise. For the frequency comparison this implies

$$\sigma_{yA-yB}^2(N_c T_c) \approx \frac{\sigma_{x-linkA}^2(T_m)}{(N_c T_c)^2} + \frac{\sigma_{x-linkB}^2(T_m)}{(N_c T_c)^2} + \frac{\sigma_{x-Sc}^2(T_c/2)}{N_c (N_c T_c)^2}$$

for N_c cycles. The resulting performance is rapidly dominated by the link flicker noise leading to $\sigma_{yA-yB}(\tau) \approx 1 \times 10^{-13}/\tau$ irrespective of the onboard clock. For a single period of common satellite visibility (0.25 days) this leads to a ground clock comparison with an uncertainty of about 5×10^{-18} in relative frequency. When allowing for several periods of common visibility, using the phase noise on each period ($\approx 10^{-15}$ s) we deduce that two periods (separated by about 2 days) are enough to reach the sub- 10^{-18} level in ground-ground frequency comparison. Note that this requires 10^{-15} s stability of onboard delays (cables, mechanical, etc.) for times up to a few 100 s ($\approx T_c$) but not for 0.9 days, as slow variations cancel to a large extent in the “switching”.

Implementation: A PRN (Pseudo Random Noise) code at ≈ 1 GHz is derived from the RF clock signal and encoded on the optical carrier. The delay of the incoming code is measured with respect to the outgoing one, and thus the onboard clock. In addition to operation as the optical link, the Tx laser is also used as the seed laser for MOLO. This allows saving cost weight and power and provides high stability for the LCT emission frequency.

The pointing requirement of the telescope is determined by the diffraction limited divergence of the telescope to be about 5.4×10^{-6} rad ($\approx 1.1''$), with actual in-lock pointing in the existing LCT well below that

level (sub μ rad).

Key parameters [Gre10, CDF10]: 125 mm telescope diameter, wavelength: 1064 nm, transmit power 2 W, mass 50 kg, electrical power 160 W, volume 0.6x0.6x0.7 m³. Transmit power can be increased to 3-5 W without additional mass and electrical power, if needed.

Current heritage and TRL: The optical link concept for STE-QUEST is making use of existing flight hardware developed by TESAT-Spacecom GmbH for the Laser Communication Terminal (LCT) presently flying onboard the German TerraSAR-X and the US NFIRE satellites [Gre10], with only minimal modifications. The overall TRL is thus very high, estimated at TRL=8/9 except for the code delay measurement estimated at TRL 4 (ACES MWL heritage).

Proposed procurement approach: TESAT

E.2.8 XPLC

The XPLC is the on-board computer that ensures control, monitoring, telemetry, and telecommand management for all EGE instruments and equipment. Besides the standard function of an on-board computer, XPLC plays a major role in EGE operations since it is directly involved in the servo loop signals generation and distribution.

All telecommands are dated when leaving XPLC. Similarly, the computer defines a time tag for all telemetry data when entering XPLC.

Current heritage and TRL = 8, from ACES development.

E.2.9 Auxiliary units

The Attitude and orbit control system (AOCS) on the STE-QUEST spacecraft will provide real-time attitude data primarily for the orientation of the spacecraft (with accuracy of 0.3° in real-time) and the proper reduction of the GNSS/SLR data. The CDF study has suggested using a system similar to the AOCS in Sentinel3, which are also resistant to radiation at GEO orbit level. TRL 7-9. See below for the actuators.

Proposed procurement approach: SODERN, SELEX, TNO.

The GNSS Receiver is used for the Precise Orbit Determination (POD), time and frequency transfer, coarse positioning (< 1 m) for real time use by the Attitude and Orbit Control as well as the back-up for time tagging of all payload data. For the time and frequency transfer, the STE-QUEST GNSS receiver is nominally using onboard reference clock frequency. The receiver assembly consists of 3 POD-antennas: one choke-ring primary in the zenith direction (for POD in perigee), and high-gain helix antenna with 45° field of view in nadir and aft looking direction (POD in apogee). By the year 2015 we can expect more than 100 GNSS satellites (GPS, GALILEO, GLONASS, COMPASS) to be available for precise orbit determination, and that should be far enough to get the STE-QUEST orbit accuracy on the level of 1-2 cm RMS for altitudes up to some 10 000 km. Using only signal from GPS satellites, the Low Earth Orbit (LEO) can be determined with an accuracy of 1-3 cm based on reduced-dynamic or kinematic POD approaches, see [Sve05]. For the orbit altitudes between 10 000 and 40 000 km, GNSS signal can only be received very shortly when a GNSS satellite is passing behind the Earth, facing the Earth and the EGE satellite at the same time, and making use of the antenna side lobes. When the EGE satellite is in apogee POD will be based on the GNSS measurements from the high-gain helix GNSS antenna as well as ranges provided by the EGE microwave/optical link. By combination of these two measurements we assume that accuracy of about 10 cm can be guaranteed. SLR measurements will be used only for independent orbit validation.

The STE-QUEST GPS/Galileo receiver would have to support three frequency bands (L1/E1, L2, L5/E5) and to enable dual frequency measurements from both constellations. Both commercial-off-the-shelf (COTS) and fully space qualified receivers are considered viable options for the STE-QUEST GNSS receiver and endorsed by ESA. A trade-off between cost, reliability and added science value needs to be performed.

Proposed procurement approach: Candidate COTS receivers include the Septentrio PolaRx receiver with timing option and the next generation JAVAD boards. The Austrian Aerospace dual-frequency GPS receiver presently developed for the 2010 SWARM mission is considered as a suitable alternative.

E.3 Alternative approach with an optical atomic clock (alternatively to PHARAO)

An optical clock based on neutral strontium atoms trapped by laser light at the time of writing it has achieved in a European laboratory a stability of 6×10^{-17} , more than a factor 10 better than the PHARAO clock will have in space, and a comparable accuracy. In addition, a breadboard cold atom source has been demonstrated under ESA support and its development towards a full breadboard clock will take place in a EU-FP7-SPACE project (2011-2014).

An alternative approach is provided by an ion clock, in which a single atomic ion is trapped and laser cooled. Ion clocks based on Sr⁺ and Yb⁺ are operational in Europe with accuracies as low as a few parts in 10¹⁶, comparable to PHARAO, but with much higher stability as well.

E.3.1 Description and key characteristics.

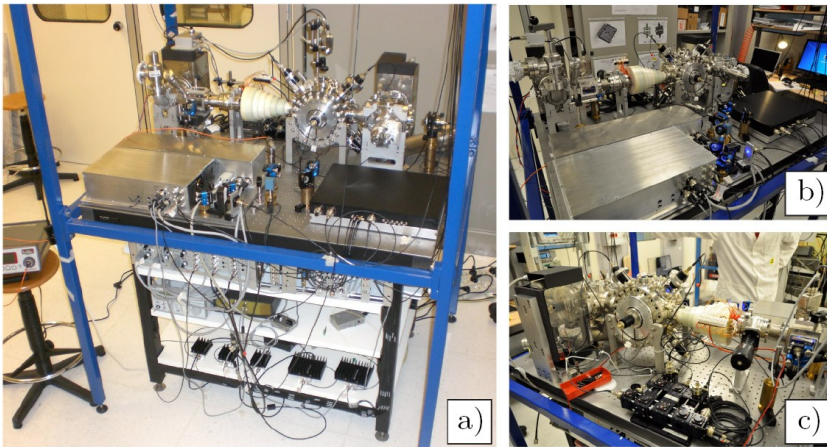


Figure E14: Current status of the transportable (120 cm × 90 cm) cold strontium source from different points of view (LENS/Università di Firenze). a) Total view of the setup showing the “physics module”. The white cone is the Zeeman slower. The metal box in the left front corner contains the 461 nm cooling laser, the black box is the frequency generation breadboard. The console hosting all the electronics for the experiment operation and control is below the breadboard. b) Front view of the physics-module. c) Rear view showing in the foreground the dichroic fiber port cluster.

The Strontium neutral atom optical clock is based on a large number of ⁸⁷Sr atoms (on the order of 10⁵) confined in an optical dipole trap within an ultra high vacuum (UHV) chamber, and laser-cooled to few microkelvin temperature. Due to the low temperature of the atoms and the appropriate choice of the wavelength of the trapping laser, both the first order Doppler and the AC Stark effects will not affect the accuracy of the frequency reference. Under these conditions, the narrow-linewidth 5 ¹S₀ → 5 ³P₀ clock transition at 698 nm can be interrogated with high fidelity by a spectrally narrow and stable clock laser source. The clock laser is a semiconductor laser diode, frequency-stabilized against the MOLO. The clock transition spectral profile is observed by stepping the clock laser frequency (electronically by changing the frequency offset in

the frequency stabilization unit), and recording the fraction of the atoms excited in the upper clock state as a function of this frequency. The clock laser is stabilised to the clock transition by repeatedly stepping back and forward between the half-intensity points on the clock frequency profile, monitoring the excitation imbalance between these points and servo-correcting any detected imbalance to zero by means of feedback to the frequency offset.

The relevant cooling, auxiliary and clock transitions wavelengths are provided by diode lasers, operated in fundamental or frequency doubled mode.

Performance assessment The ⁸⁷Sr ¹S₀ → ³P₀ clock transition at 698 nm provides a performance that will significantly enhance the accuracy of the redshift test. The stability specification for the advanced STE-QUEST is 1.5x10⁻¹⁵ /τ^{1/2}, reaching a flicker floor of 2x10⁻¹⁷. Figure E13 shows the results of the combined stability of two Sr clocks operated at SYRTE (Paris). The STE-QUEST specification is a factor of 2 below the current laboratory level, which is expected to be improved further in the next few years.

Systematic effects that affect the absolute frequency of the Sr lattice clock are understood to a large extent, and have been characterized on European Sr clocks (SYRTE, PTB [Lisdat 2009]) and a US clock [Campbell 2008]. The two Sr clocks operated in Paris agree to within 2x10⁻¹⁶. The specification for the uncertainty of the STE-QUEST clock is 5x10⁻¹⁷. This is the goal level for ongoing breadboard developments until 2014 (see below), and it is expected that this can be well achieved in a space clock.

Frequency stabilization unit consisting of several beat units (photodetectors) in which fractions of the laser waves of the different lasers are overlapped with radiation of the frequency comb to produce beats, and signal processing units to stabilize their frequencies.

Resources: For a space lattice optical clock we estimate: power 152 W, volume 135 l, mass 105 kg, including the frequency stabilization unit described below.

Operating modes The lattice clock will operate under processor control providing the control algorithms for the integrated pulse sequencing for cooling, repumping, clock interrogation, magnetic field switching and stabilization, cooling fluorescence monitoring. The controller will also provide error flags for critical processes and system reset and correction where necessary. Automatic monitoring of laser power and spectral quality, with signal re-optimisation or laser failure determination is required. All the lasers will be actively stabilized by the MOLO system. Redundant laser units will be pre-aligned and multiplexed into the fibre delivery to the trap so that redundant units can be readily activated in the case of diode laser failure.

Calibration requirements The optical clock permits on-board calibration, using the MOLO as short-term ultrastable flywheel, and the technique of interleaved interrogation [Lisdat 2009]. Furthermore, the

optical link with its excellent performance, allows performing calibration of systematic effects using ground clocks as references. Of course, this direct calibration can only be performed at the level at which the gravitational redshift is known from other measurements.

Current heritage and TRL The ^{87}Sr lattice clock structure and specifications are based on existing laboratory expertise present in Europe (LENS, SYRTE, PTB) and at JILA (USA). However, many components of a future space optical clock unit have a higher TRL as they are similar to components used in PHARAO (external cavity diode lasers, acoustooptic modulators, fiber, shutters, vacuum housing, pump, crystal optic components). Here TRL is up to 8.

TRL of the frequency stabilization unit: the beat distribution units, the virtual beat generation and the error signal generation are standard commercial components of combs or common in frequency metrology labs. They are similar to those components contained in the MOLO. There is no difficulty in reaching TRL 5 by 2014.

As a first step towards a space clock, in the ESA-ELIPS 3 project "SOC" a compact breadboard was developed with the design goals of modularity, reliability and low power consumption (Figure E15) [Schioppo 2010]. The result is a system with 210 liter volume (excluding the non-optimized electronics and supporting plate), representing a reduction in volume of a factor of about 10 with respect to a standard stationary system, 120 kg mass, and 110 W power consumption (including 20 W for electronics and 40 W for the magnets).

An EU-FP7-SPACE project ("Space Optical Clocks 2") has the goal to further develop the above breadboard, demonstrating a performance at the STE-QUEST specification (Instability $< 1 \times 10^{-15}/\tau^{1/2}$, inaccuracy $< 5 \times 10^{-17}$) by end of 2014, with TRL 4. The breadboard mass will undergo a further significant reduction compared to the present one, to 148 kg (this value is without electronics, without reference cavity for the clock laser (which would be part of MOLO), without support plate).

Procurement approach and international partners We propose to develop the optical clock up to TRL4 and to TRL5 for critical components by 2014 using funding from various sources (national and ESA GSTP). If the STE-QUEST mission is selected, and the optical clock is deemed suitable, the EM development shall be funded by national agencies.

Critical issues The appropriate laser diodes for the lasers and of necessary nonlinear crystals must be space-qualified. If serious difficulties would arise in the procurement of suitable laser diodes, an alternative optical lattice clock is provided by using Ytterbium instead of Strontium. The basic architecture of the clock is the same, the atomic properties are similar, but the laser technology is different, with fewer lasers and more space technology heritage [Ramecourt 2010], TESAT) and telecom heritage.

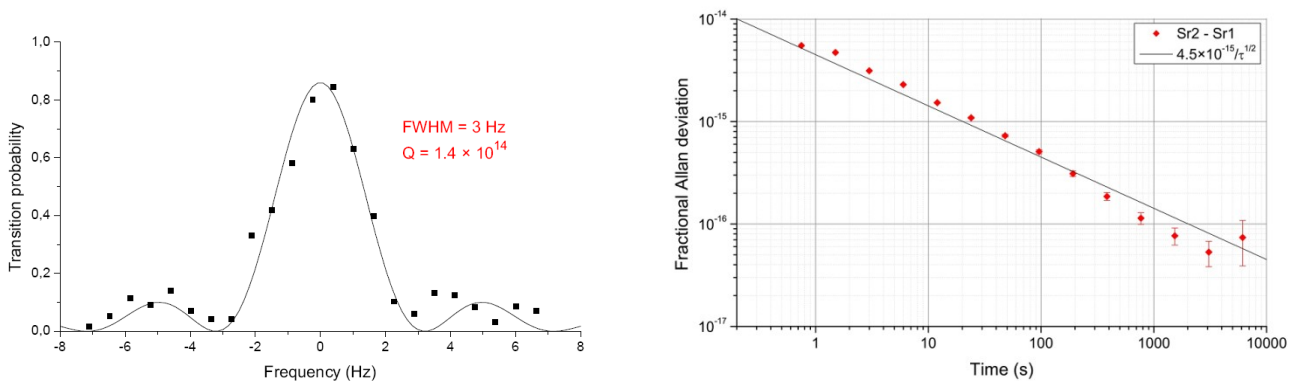


Figure E13: Left: resonance line of ultracold Sr atoms at 698 nm in an optical lattice. The line has a quality-factor Q of 1.4×10^{14} . Right: instability of the Sr optical clock pair. The instability of a single clock is a factor $2^{1/2}$ smaller, dropping to less than 1×10^{-16} (SYRTE, Paris).

F System requirements and spacecraft key issues

F.1 Number of spacecraft

For the STE-QUEST payload a single one drag-free spacecraft is required.

F.2 Attitude and orbit control required: spinner/scanner/3-axis stabilized and associated requirements

Pointing is Nadir-pointing with yaw steering. Pointing requirements are not stringent in this mission (0.3 deg), since the OL and the MWL are able to reach the ground targets. No need of a drag-free control system.

As actuators, the CDF study has suggested thrusters, reaction wheels (Rockwell Collins), and optionally magnetotorquer bars (their location can be sufficiently far away from the atomic clock so that its magnetic field is not perturbing, but they are useful only near perigee).

Vibrations induced by the wheels are much less of concern than the solar arrays driving mechanism.

Orbit control: The CDF study has indicated that for the proposed orbit, one Delta v manoeuvre every half year, in the range up to 41 m/s is required to maintain the orbit. Two 41 N thrusts are foreseen to this end.

F.3 On-board data handling and telemetry requirements

The on-board data handling (OBDH) system is characterised by the continuous acquisition of a low data rate from the payload instruments. The OBDH is also in charge of storing the science data during ground station non-visibility for later downlink. The TT&C Transponder could be based on existing hardware (SWARM) with 7 W of power.

Science data rate is on the order of 45 kbps generated on the instruments (5 kbps housekeeping, plus 40 kbps science data). The downlink approach envisages onboard storage of 324 Mbyte per orbit or 486 Mbyte per day. A 2 Gbyte mass memory will be required to store the data acquired between successive downlink sessions. Commercial S-band ground stations (13 m dishes) can accommodate this.

F.4 Mission operations concept (ground segment)

The ground segment is composed of:

- 1.) Mission control is by an ESA control station that directs satellite bus and orbit manoeuvres,
- 2.) Payload control, will be performed from a payload control station. This could be an evolution from the ACES control station located at CNES Toulouse. It also receives data from the ground clock network and from the laser ranging stations acquiring data for the orbit determination. It interacts with the ESA control station.
- 3.) Ground optical clock network (minimum 2 clocks on different continents, each with MWL terminal and ground OL), transmitting their data to the ESA control station.
- 4.) Existing laser ranging stations worldwide (ILRS), transmitting data to the Payload control station

F.5 Estimated overall resources (mass and power)

This summary is based on the CDF assessment study (16.7.2010, file "Systems_IFP_final2.ppt").

<i>Unit</i>	<i>Mass [kg]</i>	<i>Power [W]</i>	<i>Comment</i>
Payload module			
PHARAO	91.0	113.5	2.5 W in safe mode
Communications (Microwave link MWL)	18.0	71.5	Ka and S-bands only
Optical link (based on LCT)	50.0	160.0	
Atom interferometer	50.0	25.0	Power value shown is additional power needed in interferometer mode compared to clock mode
MOLO:			
- Reference cavity	15.0	23.0	
- Optical frequency comb	16.0	17.0	
-Electronics		20.0	
FCDP	8.0	8.4	
GPS receiver	8.5	7.0	
CCR	2.0	2.0	
Structure	69.4		
Thermal control	11.3		
Mechanisms	0.9		
Data Handling	13.6		
Harness	11.5		
ICU/PDU		175.0	
Payload sum	315.0	621.4	
Payload module sum incl. individual	408		

margins			
Service Module			
Structure	118.6		
Thermal control	9.0		
Mechanisms	12.1		
Communications	7.6		
Data handling	7.7		
AOCS	41.1		
Propulsion	16.7		
Power	93.2		
Harness	29.9		
Service module sum	335.0		
Service module sum incl. individual margins	373.0		
Payload plus service module, incl. 20% system margin	927.0		
Propellant	61.0		
Launch adapter	110.0		
S/C launch wet mass incl. all margins	1098.0		
Optical clock (incl. atomics package, clock laser, auxiliary lasers, laser frequency stabilization unit, clock control electronics)	105.0	152.0	Alternative clock to PHARAO

The total satellite wet mass including margins is far below the allowable limit on a Soyuz launch of 1633 kg.

Advanced STE-QUEST scenario: the replacement of PHARAO by an optical clock (adding 17 kg + 40 kg and. 40 W + 40 W (the second contributions coming from the kept PHARAO laser bench) are not critical can be accommodated by a modest increase in the solar array size.

F.6 Specific environmental constraints

The instruments will be located in the satellite structure such as to realise ionizing radiation shielding by the spacecraft structure and non-sensitive equipments to the maximum extent possible; the need for additional radiation shielding (including trapped proton radiation) for especially sensitive parts of the instruments must be studied. It should also be mentioned that an orbit with higher perigee and less radiation dose is also an option, as it leads to a tolerable reduction of the science goals.

Allowed temperature range is +10 °C - +30 °C. The required $\pm 2^\circ\text{C}$ temperature stability over 1 orbit at the interface to the payload enclosure is feasible. The thermal control will employ the usual means (an enclosure with high thermal inertia, heaters and a suitable radiator). The location of the radiator will need a special study given the non-standard orbit.

A magnetic field present during the mission can affect the properties of the onboard clock. Using SPENVIS, the magnetic field has been calculated along the spacecraft orbit: the field intensity presents maxima around 0.2 gauss and a minimum values of the order of 10^{-3} G. As discussed above, this is not a limitation to the instrument performance.

Microvibrations: $< 8 \mu\text{g Hz}^{-1/2}$ in the range 2 mHz to 10 Hz, so as to minimize perturbations of the optical cavity in the MOLO.

Radiation: 30 krad. Equipment specified for GEO can be used as is; equipment specified for ISS usage must receive a 3 mm thickness Aluminium shield. This is planned on the payload box.

F.7 Current heritage (assumed bus) and technology readiness level

The satellite bus design drivers are: nadir-pointing microwave antennas and LCT, thermal stability for the payload instruments, no strong magnetic sources at the clock location, low micro-vibrations, harsh radiation environment due to crossing of the radiation belts once per orbit, power demand by science payload (with the possibility to reduce power demand by stand-by of some components during specific mission phases, e.g. eclipse), mass limit due to required high altitude with low cost launch.

The satellite is modular, being composed of a payload module and a service module. The CDF Study considered a modified PROTEUS satellite as the service module as a zero-order approximation. Modifications include the use of attitude control thrusters, larger tanks for the propellant used in orbit

maintenance, extra shielding against radiation. The solar arrays are deployable and rotating. It was checked that the micro vibrations generated by the driving mechanism are within the required level.

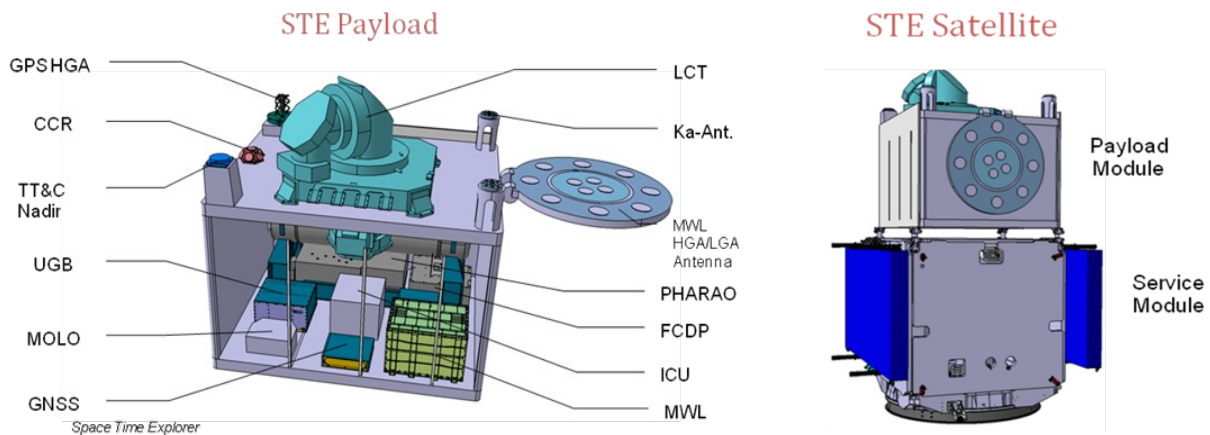


Figure F1: Schematic of the payload module (left) and of the complete satellite (right), according to the CDF study by ESA. For the STE-QUEST mission, an additional payload module, the AI including its laser will be added.

F.8 Proposed procurement approach & international partners

The procurement has been proposed in the subsections on the individual payload components.

For the ground segment, we foresee at least one international partner, that will operate an optical clock on ground with their respective optical and MWL terminals.

Baseline: 1 station in US (e.g. National Institute of Standards and Metrology, Boulder).

The establishment of at least 1 station in Europe will be ensured, as several optical clocks are being developed in Europe (UK; F, D, I) and at least one will be available for the STE-QUEST mission

More stations (e.g. Japan plus one transportable station operated by a European consortium) are desirable

F.9 Critical issues

All critical issues were described in the instrument section.

G Science Operations and Archiving

G.1 Science Operations Architecture and proposed share of responsibilities

A STE-QUEST Science Master Plan will be prepared by the Science Team. The detailed planning for the operations of the payload will be developed by the Payload control team, some members of which are also members of the Science Team. The payload control team will interact with the Mission Operations Team at ESOC. Science operations will be implemented by the Payload control team under the responsibility of the ESA Project Scientist, with strong support from the Specialist Teams (members of which have participated in the instrument developments). This includes the preparation of the experiment sequences and timelines to be supplied to the Mission Operations Team for integration into the overall spacecraft operation timeline. The detailed plans for the science operations will be documented in the Science Management Plan to be approved by SPC after mission selection.

G.2 Archive approach

Data exploitation is primarily the task of the PI teams, coordinated within the Science Working Teams (SWT) by the Project Scientist, as appropriate. A twofold approach is proposed. First a quickly available set of survey data will be defined and made public on the World Wide Web in the form of key Parameters. Second, data will be calibrated and prepared by all PIs according to tested formats for distribution. Archiving will be based on the data sets prepared by the PI teams, with the agreed and tested formats and access software. Assembly of these data sets into an ESA archive for use by the wide scientific community will be the responsibility of the Science Operations Team (see „Data Rights“ section below). Archiving of the data is the responsibility of the PIs who will ensure that the complete data set remains accessible after the end of the mission. A central facility may be identified in one of the ESA member states that would be used to store and maintain the data sets and software tools for later exploration.

G.3 Proprietary data policy

STE-QUEST data rights are based on the established ESA “Rules concerning information and data”, as defined in ESA/C (89)95. First publication rights for data obtained by a PI investigation reside with the PI team for six months from receipt of the original science telemetry and auxiliary data (e.g. orbit attitude and space craft status information) After this time, data will become available to the scientific community at large.

The PI teams will provide ESA with processed and usable data for Public Outreach (PO) purposes as soon as possible after their receipt The PI teams will also support a PO Plan that will be provided by ESA in due time. The PI teams will provide records of processed data with all relevant information on calibration and instrument properties to the ESA Archive System. The data Format shall be compatible with those defined for ESA Archive System.

Scientific results from the mission will be published, in a timely manner, in appropriate scientific and technical journals. Proper acknowledgment of the services provided by ESA will be made.

H Technology development requirements

H.1 Payload TRL level and technology development strategy

H.1.1 Critical issues

The CDF study of the STE-QUEST mission has identified several high risks. Here we comment on them and their reduction:

- 1.) **Low TRL of MOLO:** A frequency comb for operation will be flown in a sounding rocket by end 2013. This will drive the TRL up substantially to 7-8 by 2014. The space company SODERN is developing together with SYRTE an engineered version of a reference cavity to be tested in 2011. It will also be tested in an optical clock in the framework of EU-FP7 project “SOC2”. More compact and robust reference cavities are under development in other labs such as PTB. A development program aimed at demonstrating a complete MOLO in a relevant environment by 2014 should be initiated in 2012 so that TRL 5 will be demonstrated by 2014.
- 2.) **End-to-End MWL:** Results on the ACES MWL link in space will become available by 2014-15. An EM of the upgraded MWL for STE-QUEST could be developed rather soon an end-to-end tests performed in the field or in test setups.
- 3.) **Failure of PHARAO to meet obsolescence/evolution requirements:** The price given above for the PHARAO instrument takes into account the proposed evolution. As several critical components, such as the acousto-optical modulators or the laser diodes, and many more components in the electronics will need to be changed for PHARAO to be able to fly in 2022 due to obsolescence of components, as well as a higher level of radiations, it is favourable to use this situation to change the operating wavelength of PHARAO to that for Rubidium instead of Cs. Therefore there will be some minor re-design choices and the associated qualification programs.
- 4.) We expect that the experience acquired in previous qualification program of PHARAO will save a lot of effort in the qualification of new, but similar components.
- 5.) **Extended mission duration with respect to Payload Reliability:** Indeed, a Reliability Assessment Plan must be developed
- 6.) **Impacts due to Overly Complex Project Organisation:** The project could be run by ESA, similar to ACES. A science committee, evolving from the ACES science committee, will interface with ESA. This makes sure that the scientific and project organisation ability heritage is maintained.
- 7.) **Loss of ACES Heritage technical resources and skills:** Can be avoided by an appropriate development program, which includes e.g. combining the PHARAO engineering model with a laboratory version of a MOLO and characterizing it, developing an improved cold atom source for PHARAO, upgrade of MWL to the specs of STE-QUEST and ground tests over multi-kilometric distances.
- 8.) **Single Point Failures in Payload Supply Chain:** These are to be identified.
- 9.) **Optic fiber performance in HEO not demonstrated:** Tests are being performed in the framework of DLR project “FOKUS”

H.1.2 Main technology development requirements (2011-2014):

- 1.) Develop improved subsystems for PHARAO, in particular its atom source, to increase its frequency stability
- 2.) Continue ongoing developments of the optical frequency comb towards long-term operation in space (follow-up of ongoing DLR project "FOKUS")
- 3.) Continue ongoing developments of ultra-high finesse reference cavities and other optical clock components for space (planned in an ESA GSTP (2011-2013), to be followed by further activities)
- 4.) Demonstrate complete MOLO working in a relevant environment
- 5.) Development program for demonstrating high-accuracy frequency comparisons via OL (CNES, DLR activities, ESA activity ITT 6404, 2010)
- 6.) Develop the STE-FCDP starting from the ACES - FCDP
- 7.) Demonstrate AI with BEC and long interrogation times in relevant environment (CNES, DLR activities in the I.C.E., QUANTUS and MAIUS missions)
- 8.) For STE-advanced: Further technology development and qualification program for optical components for optical clock, in particular laser diodes and nonlinear-optical crystals (initial steps will be taken in the GSTP project; additional activities are needed, in particular concerning the atomics package).

H.2 Mission and Spacecraft technology challenges

No particular challenges are seen for the spacecraft. Concerning the instruments, the critical issues have been described above.

I Preliminary programmatics/Costs

I.1 Overall proposed mission management structure and programme schedule

Study and technology development phase (2011-2014): The proposing science team (p.2), with members from all main quantum physics institutes in Europe, will follow STE-QUEST in case of selection for Phase 0. In particular, the Science Team will include specialists for the various aspects of the payload, the link modelling, and the orbit characterization. They will assist ESA and industry during the feasibility studies.

The Science Team can be extended to persons from additional research labs, including from people from the geophysics/geodesy community. The Science Team will have a strong overlap with the ACES Science team, ensuring the experience is taken over. Members of the Science Team will in part be personally involved in the ongoing development of the technology and ground tests required for STE-QUEST

The actual selection of the clock type (whether or not to opt for the advanced STE-QUEST scenario) will depend on the outcome of the studies on optical clocks, which will also provide a detailed cost feasibility analysis. These studies will be ongoing in the science team in the coming years, and will complement ESA's phases o/A and definition phase A/B1.

EM, FM, and ground station development phase (2015-2022): In this phase the Science Team will provide input and participate in calibration and testing infrastructure at the subcomponent, subsystem and system level. It will also continue to consult and perform and specialized analyses (modelling/measurements) for industrial development work and participate in reviews. To enable this, the Science Committee will set up Specialist teams, which will include:

- Clock calibration, Interferometer calibration, - MWL & Optical link ground segment maintenance, - MWL calibration, - data analysis, - laser ranging, - orbit determination, TT&C, - data archiving and dissemination, - system modelling, - geophysics measurements, - interface to institutions (metrology labs, climatology labs, geodesy community), - communications and outreach. The Specialist teams will evolve out of the teams already established in the framework of the ACES mission, and who have developed significant know-how.

An important activity by the Science Team will be to supervise the establishment of the Payload control center and to select the personnel for it.

A Mission Planning team with representatives from each Specialist team will also be created and develop the mission operational concept. During the FM development phase, a Daily Operations team will develop detailed procedures for use during the mission phase.

The ground station receivers with respective optical clocks/optical links are an integral part of the mission; they will be user-furnished, and operated outside the programmatic frame of ESA.

Mission phase (2022-2027, with possible extension): Operations will be under the responsibility of the payload control team following the plan developed by the Mission Planning team. Concurrently, the Specialist teams will be monitoring the instruments, and performing preliminary data analyses.

Science analysis phase (2022 onwards): In cooperation between several Specialist teams, the mission data will be fully analyzed and the results prepared for public dissemination.

I.2 Preliminary risk analysis

There are two main risks associated with the main payload items

(1) Conversion of PHARAO from Caesium to Rubidium encounters technological difficulties.

Downscoping solution: use PHARAO with Caesium, as in ACES, or use the optical clock, if available.

Consequences: accuracy of Earth redshift measurement is reduced by a factor corresponding to the lower accuracy of the clock, approximately 3. The Solar redshift measurement is not affected.

If the technological difficulties are related to the laser system for Rubidium, this would also entail dropping the atom interferometer.

Approach for minimizing risk: technology research program will include parallel activities on different types of laser diodes produced by several European and non-European manufacturers

(2) Atom interferometer encounters technological difficulties.

As the atom interferometer and Rb clock payloads uses the same technologies, the main risk is coming from the production of the BEC. The two possible technologies (atom chip or dipole trap) have been demonstrated in laboratories. The two equipments have also been tested in micro-gravity: with drop tower for the atom-chip and in 0-g plane for the laser.

Downscoping solution: omit this instrument from mission.

Consequence: no test of the Weak Equivalence Principle possible, but savings in cost (no EM and FM). Clock measurements are not affected.

Approach for minimizing risk: The use of two different technologies and of other possible lasers (different wavelength) for the dipole trap reduces the risk. The space qualification of these devices has to be investigated in priority. The use of Nd-YAG laser is a back-up solution as it has been demonstrated yet in laboratory. In this case, the Nd:YAG laser of the LCT could be used, saving cost and mass.

I.2.1 Preliminary Payload/Instrument Cost Analysis

Costs to ESA:

Spacecraft, launch and satellite operations costs have been estimated during the CDF study on STE-QUEST to be less than the 470 M€ cost to ESA envelope of a Cosmic Vision Mission. The exact cost has not been made public yet.

We propose that ESA covers the spacecraft bus plus the microwave clock, links and associated payload (FCDP, GNSS, etc.), as well as mission control via ESOC. The rationale for this is that the technology of clocks and links are strategic and will be widely applicable in future ESA missions and programmes (spacecraft ranging, geodesy from space, spacecraft formation flying), well beyond the fundamental physics studies that are the goal of the STE-QUEST mission. The cost of a PHARAO flight model based on Caesium had been estimated in the CDF study with 40 M€. However, the CNES estimates 20 M€, including changes required due to obsolescence of components. As this work can be efficiently combined with a change from Caesium to Rubidium and implementation of an atom source with more atoms, we estimate the total cost of a FM of PHARAO-Rb to be below 30 M€ This is well within the 40 M€ for the microwave clock assumed in the CDF assessment study, and thus the overall cost to ESA does not increase.

Non-ESA costs:

(1) The development costs for the technology required for the clock aspect of the mission, including test campaigns, are 10 M€ (PHARAO-Rb: 5 M€, optical link ground and space segment, 2 M€; MOLO: 2 M€, MWL and FCDP: 1 M€)

(2) Atom interferometer: 40 M€ (technology development, EM and FM construction)

(3) Pre-mission ground segment:

Payload control ground station development (Europe) 5 M€ (based on the ACES ground segment)

European Optical clock ground station development: 2 M€ (using an ILRS receiving station;

US Optical clock ground station development:	incl. MWL ground terminal) 6 M€ (of which 5 M€ are the cost of LCT ground terminal, 0.3 M€ for MWL)
<i>Optional:</i> Japanese Optical clock ground station develop.:	6 M€ (as above)
<i>Optional:</i> transportable optical clock ground station	2 M€ (optical clock plus MWL)
(4) During mission, ground segment:	
Payload ground station operations	6 M€ (5 years, incl. archiving, etc.)
European Optical clock ground station operations	2 M€ (5 years)
U.S.A. Optical clock ground station operations	2 M€ (5 years)
<i>Optional:</i> Japanese Optical clock ground station op.	2 M€ (5 years)
Laser ranging station operating costs	- (covered by running budgets)
<i>Optional:</i> transportable ground station operations with ~ 50 relocations	6 M€ (5 years)
(5) Post-mission, ground segment:	
Data analysis	- (covered by national agencies through grants)
(6) <i>Optional:</i> optical clock: 40 M€ (only in case that the advanced STE-QUEST scenario is selected and the space optical clock is to be built) for technology development, EM and FM construction)	

I.3 International partners

For the ground segment, we foresee at least one international partner, that will operate an optical clock on ground with their respective optical and MWL terminals.

Baseline: 1 station in US (e.g. National Institute of Standards and Metrology, Boulder).

More stations (e.g. Japan plus one transportable station operated by a European consortium) are desirable.

J Communication and Outreach

This mission is very clear in its proposed goal, and it can be communicated very well to the general public. This also holds for the geophysics spin-off that can be obtained from the mission. Furthermore, the technological aspects of the mission are ground-breaking for future time-keeping and reference frame systems in space, and thus are also expected to be of interest to society at large.

The proposing team encompasses a large fraction of the European scientific community in the field of quantum metrology and a number of European geophysics groups that can benefit of the resources that STE-QUEST can provide. After preselection of the mission, we will seek to enlarge the user group further.

Communications will be handled at different levels using different media and includes a continued presence at general and specialist conferences and workshops, popular science magazines and space activities magazines. A STE-QUEST web site will be designed and maintained by the ESA Science Communication Division. It will include the links to the experiment web pages and will be updated and developed following the input and advice of the STE-QUEST Science Working Team and Project Scientist and Manager. A dedicated science journalist will be selected for the project and will support the Project Scientist and Manager for science communication, public outreach and the related activities.

K References

- [Ash07] N. Ashby et al., PRL 98, 070802 (2007)
 Bar01] Barrett et al., Phys. Rev. Lett. 87, 010404 (2001); Grimm et al., ADV. IN AT., MOLEC. AND OPTICAL PHYS., VOL. 42
 [Ber01] B. Bertotti et al, Nature 425, 374 (2003)
 [Bje85] Bjerhammar, A. (1985) Bulletin Géodésique, 59, 207.
 [Bla00] L. Blanchet et al., Astron. Astrophys. 370, 320 (2000).
 [Boy07] Boyd et al, PRL 98, 83002 (2007).
 [Cas96] Y. Castin, R. Dum, Phys. Rev. Lett. 77, 5315 (1996).
 [CDF10] ESA Space-Time Explorer Assessment Study, final presentation pp. 84-94, <http://sci.esa.int/science-e/www/object/index.cfm?fobjectid=47559#>
 [Cle09] Clément et al, Phys. Rev. A 79, 061406(R) (2009)
 [Dam02] T. Damour, F. P. & Veneziano, G., PHYSICAL REVIEW D, 2002, 66, 046007

- [Dau05] C. Daussy, et al., Phys. Rev. Lett. 94, 203904, (2005).
- [Deg02] J. J. Degnan, J. of Geodynamics 34, 551 – 594, (2002)
- [Den04] S. Dent, et al., arxiv:0705.0696; V.F.Dmitriev, et al., Phys. Rev D69,063506(2004) and refs. Therein.
- [Dje10] P. Wolf, et al., Proc. Int. Conf. on Space Optics, session 13b, <http://www.icsoproceedings.org/>, (2010). K. Djerroud, et al., Opt. Lett. 35, 1479 (2010).
- [Duc09] L. Duchayne et al. (2009). A&A preprint, DOI 10.1051/0004-6361/200809613.
- [Fla07] V.V. Flambaum, arxiv:0705.3704.
- [For07] T.M Fortier et al, PRL, 98, 070801 (2007)
- [FTK] V.V. Flambaum, M.G. Kozlov, Phys. Rev. Lett. 98,240801(2007); E. Reynold et al Phys. Rev. Lett. 96, 151101(2006); T. Tzanavaris et al Phys. Rev.Lett. 95,041301(2005); N.Kanekar et al Phys. Rev. Lett. 95, 261301(2005).
- [Fu01] Fu, L.L., Cazenave A. (2001), "Satellite Altimetry and Earth Sciences" (Academic Press)..
- [Gre10] M. Gregory et al., Proc. Int. Conf. on Space Optics, session 8a, <http://www.icsoproceedings.org/>, (2010).
- [Hof61] B. Hoffmann, Phys. Rev. 121, 337 (1961)
- [Hos05] K Hosaka et al. 2005,IEEE Trans. Instrum. Meas. 54 759 (2005)
- [IER03] IERS TN 32 (2004), Verlag des BKG; G.H.Kaplan, astro-ph/0602086.
- [Jia08] H. Jiang, et al. J. Opt. Soc. Am. B 25, 2029 (2008). G. Grosche, et al., Opt. Lett. 34, 2270 (2009).
- [Jun08] Jung et al., Phys. Rev. A 78, 011604(R) (2008)
- [Kag96] Y. Kagan, E. L. Surkov, G. V. Shlyapnikov, Phys. Rev. A 54, R1753 (1996).
- [Kap00] Kaplan, D. B. & Wise, M. B., *JHEP*, 2000, 8
- [Kos99] A. Kostelecky, C.D. Lane, Phys. Rev. D60, 116010 (1999)
- [Kri93] T.P. Krisher, et al., Phys. Rev. Lett., 70, 2213 (1993)
- [Läm01] C. Lämmerzahl et al., Class. Quantum Grav. 18 (2001) 2499
- [Läm04] C. Lämmerzahl et al., Gen. Relativity. and Gravit. 36, 615 (2004)
- [Lem05] P. Lemonde and P. Wolf, Phys. Rev. A 72, 033409 (2005)
- [Lin02] B.Linet and P.Teyssandier, Phys.Rev. D66, 024045 (2002); C.Le Poncin-Lafitte and S.B.Lambert, astro-ph/0610463.
- [Lop08] O. Lopez, et al., Eur. Phys. J. D 48, 35–41, (2008).
- [Lop10] O. Lopez, et al. Appl. Phys. B 98, 723–727, (2010).
- [Lop91] J.C. LoPresto, et al., Astrophys. J., 376, 757 (1991).
- [Mar04] H.S. Margolis et al. 2004, Science 306, 1355.
- [MIC] <http://smc.cnes.fr/MICROSCOPE/>
- [Moy03] T.D.Moyer, "Formulation for Observed and Computed Values of DSN Data Types for Navigation" (John Wiley, New York, 2003).
- [New07] N. R. Newbury et al. (NIST), EFTF/FCS 2007.
- [Osk06] W.H. Oskay et al., Phys. Rev. Lett. 97, 020801 (2006)
- [Pet99] A. Peters, K.Y. Chung and S. Chu, Nature, 400, 849 (1999)
- [Rei05] C. Reigber, et al. J. Geodynamics, 39, Issue 1, 1 (2005)
- [Ramecourt 2010] D. Ramecourt et al., Proc. ICSO 2010.
- [Rum00] R. Rummel et al. (2000) IAG-Symposia 120, 261 (Springer, Heidelberg)
- [Sch05] T. Schneider et al., Phys. Rev. Lett. 94 230801(2005).
- [Sch07] S. Schlamminger et al., Phys. Rev. Lett. 100, 041101 (2008)
- [Sna89] M.J. Snadden, J.M. McGuirk, P. Bouyer, K.G. Haritos, and M.A. Kasevich, Phys. Rev. Lett., 81, 971 (1998)
- [Sof03] M. Soffel, et al., Astron.J. 126, 2687 (2003).
- [Sor00] Y. Sortais, et al., Phys. Rev. Lett., 85, 3117-3120 (2000)
- [SR] G. Ehlers and C. Lämmerzahl eds. „Special Relativity: Will It Survive the Next 101 Years? “ (Springer 2006); Conferences on CPT Invariance 1998, 2001, 2004, 2007, Indiana University
- [Sve05] D. Svehla, M. Rothacher (2005) Advances in Space Research 36, 376
- [Tam07] C. Tamm et al., 2007, IEEE Trans. Instrum. Meas 56, 601
- [Tap04] B.D. Tapley, et al. (2004) Science, Vol 305, 503
- [Ves81] R.C.F. Vessot et al. Phys. Rev. Lett. 45, 2801 (1980)
- [Vogt 2010] S. Vogt, C. Lisdat, T. Legero, U. Sterr, I. Ernsting, A. Nevsky and S. Schiller, arXiv:1010.2685 (2010)
- [Will93] , C. M. Will, Theory and Experiment in Gravitational Physics (1993)
- [Wil06] C. M. Will, Living Rev. Relativity 9, 3 (2006).
- [Wil76] J.G. Williams et al., Phys. Rev. Lett. 36, 551–554 (1976)
- [Wol06] P. Wolf, et al. Phys. Rev. Lett. 96, 060801 (2006)
- [Zoe10] T. van Zoest et al., Science 328, 1540 (2010)